catalysts

MDPI

Review

Understanding Hydrodechlorination of Chloromethanes. Past and Future of the Technology

Sichen Liu, Javier A. Otero, Maria Martin-Martinez *, Daniel Rodriguez-Franco, Juan J. Rodriguez and Luisa M. Gómez-Sainero

Departamento de Ingeniería Química, Facultad de Ciencias, Universidad Autónoma de Madrid, Cantoblanco, 28049 Madrid, Spain; sichen.liu@uam.es (S.L.); javier.otero@uam.es (J.A.O.); daniel.rodriguezf@uam.es (D.R.-F.); juanjo.rodriguez@uam.es (J.J.R.); luisa.gomez@uam.es (L.M.G.-S.)

* Correspondence: maria.martin.martinez@uam.es; Tel.: +34-91-497-5527

Received: 9 November 2020; Accepted: 9 December 2020; Published: 14 December 2020

Abstract: Chloromethanes are a group of volatile organic compounds that are harmful to the environment and human health. Abundant studies have verified that hydrodechlorination might be an effective treatment to remove these chlorinated pollutants. The most outstanding advantages of this technique are the moderate operating conditions used and the possibility of obtaining less hazardous valuable products. This review presents a global analysis of experimental and theoretical studies regarding the hydrodechlorination of chloromethanes. The catalysts used and their synthesis methods are summarized. Their physicochemical properties are analyzed in order to deeply understand their influence on the catalytic performance. Moreover, the main causes of the catalyst deactivation are explained, and prevention and regeneration methods are suggested. The reaction systems used and the effect of the operating conditions on the catalytic activity are also analyzed. Besides, the mechanisms and kinetics of the process at the atomic level are reviewed. Finally, a new perspective for the upgrading of chloromethanes, via hydrodechlorination, to valuable hydrocarbons for industry, such as light olefins, is discussed.

Keywords: hydrodechlorination; chloromethanes; production of olefins; production of paraffins; mechanisms and kinetics; deactivation and regeneration of catalysts

1. Introduction

Among Volatile Organic Compounds (VOCs), chloromethanes are classified as a group of monocarbon hydrocarbons where at least one hydrogen atom has been replaced by a chlorine atom. Similar to methane (CH_4), monochloromethane (MCM) is a gas at normal atmospheric conditions. Dichloromethane (DCM), chloroform (TCM) and carbon tetrachloride (tetrachloromethane, TTCM) possess common physico-chemical properties such as low flammability, high volatility, high stability and good liquid solvent capacity. Due to their particular properties, these compounds are widely used in the chemical and pharmaceutical industries as solvents, degreasing agents, dry-cleaners, adhesive components, etc. [1]. Moreover, chloromethanes are used as raw materials or intermediates in many synthetic industries, such as the production of cellulose acetate film, for which DCM is the main raw material, or the production of DCM, for which TCM is used as an intermediate [2]. As a consequence, hundreds of thousands of tons of chloromethanes are produced annually. However, due to their high volatility, large amounts of these chloromethanes are emitted to the atmosphere through liquid discharges and evaporation [1,2], negatively affecting to the environment and human health. It has been demonstrated that these four compounds are carcinogenic [3] and may cause hepatic disease [4]. Moreover, they also contribute to the destruction of the ozone layer [5], and favor the greenhouse effect and some dangerous environmental phenomena such as photochemical smog.

All these negative effects have led to a severe regulation of chloromethanes emissions. The use, production and emission of TTCM was forbidden by the Montreal Protocol in 1987 [6], a pact that was universally ratified in 2009 [7]. DCM, TCM and TTCM have been registered as a priority or blacklist pollutants by the European Regulation, the U.S. Environmental Protection Agency (EPA) and the Ministry of Environmental Protection (MEP) of China [2]. According to the European Regulation (EC) N° 166/2006, DCM and TCM air emissions must not exceed 1000 and 500 kg/year, respectively [8]. Furthermore, the U.S. EPA requires emissions of 1000 pounds (453 kg) or more to be registered [9].

In consequence, new applications to remove these compounds have emerged in the last 40 years in order to achieve these emissions' reduction. Non-destructive treatments, like adsorption, absorption or condensation, consist in the transference of the chloromethane to another phase, allowing the recovering of the compounds. However, these techniques involve economic efforts to regenerate the contaminated phase and remove the pollutant [10]. Thus, some destructive treatments have been developed, showing economic profitability and high effectiveness in removing the chloromethanes. However, some of them have several limitations. Thermal treatments require temperatures above 1000 °C to achieve complete oxidation of the chloromethane, an important economic problem. Besides, this high temperature promotes the formation of nitrogen oxides (NOx). These problems might be solved by adding a catalyst, with the associated risk of incomplete combustion and formation of highly toxic compounds (polychlorinated dibenzo-*p*-dioxins and/or dibenzofurans) [11]. On the other hand, biological treatments require long acclimation periods for the microbial population, which may take months for VOCs [10], and are limited by the pollutant concentration used [10].

Although incineration is the most studied technology nowadays, in the last 20 years, there has been a significant increase in scientific publications concerning reductive treatments, in particular hydrodechlorination (HDC), a promising technology to remove chlorinated pollutants. This technique allows reduction of the chloromethane into light hydrocarbons according to the well-known reaction

$$C_xH_yCl_z + z\ H_2 \overset{\text{catalyst}}{\rightarrow} C_xH_{y+z} + z\ HCl$$

Although HDC is not yet fully industrialized, the development of this technique through the last 10 years has shown outstanding results in terms of efficiency and pollutant removal. One of the advantages of HDC is the smooth operation conditions required (it may even operate at atmospheric pressure and ambient temperature [10]), saving energy and cost. In addition, selectivity of the process may be controlled using adequate catalyst and operation conditions, always obtaining products less hazardous than the original chloromethanes. Besides, it has been successfully used for the treatment of low and high concentrations of pollutants. There have been published several reviews about HDC, mainly regarding the HDC of chloroaromatic pollutants. Despite some of them including chloromethanes in their studies [2,12–16], they are mainly focused on their sources, remediation technologies, or are particularly interested in the liquid phase or in the use of specific catalysts. The aim of this review, therefore, is to collect in a single paper the existing information published in the literature about the HDC of chloromethanes.

2. Chloromethanes Treated by Hydrodechlorination

Figure 1 shows the publications regarding the HDC of chloromethanes in the last 25 years. Half of them investigate the HDC of TTCM, and a fourth part deals with the HDC of DCM. The rest are mainly dedicated to the treatment of TCM, since the HDC of MCM has been scarcely studied [1,17,18]. Binary or even ternary mixtures of chloromethanes have also been treated by HDC in several works [19–25].

The reactivity of chloromethanes in HDC increases with the chlorine content in the molecule as follows: TTCM > TCM > DCM > MCM. Since the first step in HDC reaction seems to be the breaking of the C-Cl bond [26], some authors [1,26,27] attributed the different reactivity of chloromethanes to their C-Cl bond dissociation energy (E_{dis}), the E_{dis} values for TTCM, TCM, DCM and MCM being, respectively, 305, 325, 339 and 351 kJ·mol^{-1} [2,26].

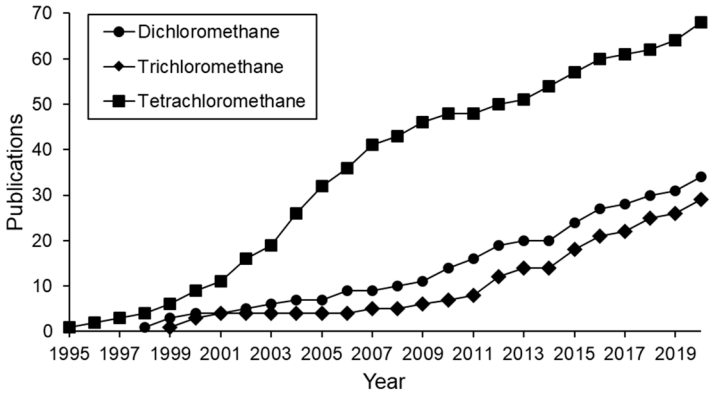

Figure 1. Evolution of publications on HDC of different chloromethanes in the last 25 years (cumulative incidence).

In the literature, the HDC technology has been used for the removal of the chlorinated pollutant or the production of valuable products from chlorinated compounds. Complete conversion and almost complete dechlorination have been achieved for DCM [1,18,20,21,23,28–46], TCM [1,18,20,21,23,27,31–34,43,47–50] and TTCM [27,50–79]. Additionally, the upgrading of residual chloromethanes for the production of valuable hydrocarbons, such as light olefins or paraffins, which could be used as feedstock in chemical and petrochemical industries, has also been explored in recent years [32–34,48]. Moreover, the HDC of TTCM has been used in several works for the selective production of TCM [53–56,80–83].

The number of publications dealing the HDC of chloromethanes increases every year (Figure 1). Since 1995, the HDC of TTCM has always caused the highest interest, although its consumption and production were forbidden after the Montreal Protocol in 1987 [6]. Nevertheless, evidence has been found of disturbing on-going unidentified TTCM emission sources [84], explaining the continued research on TTCM elimination since then. The Montreal Protocol led to a dramatic reduction in the industrial production of TTCM and its substitution by other chloromethanes. As a result, the use and release to the environment of DCM and TCM increased, becoming new environmental problems. Therefore, the number of publications concerning the treatment of DCM and TCM increased (Figure 1). DCM has been considered carcinogenic for humans since 2011, when the U.S. EPA updated its toxicology summary [3]. The same evidence was found for TCM and TTCM, which may also cause hepatic disease [4]. This emphasizes the importance of finding effective technologies to remove or transform these dangerous chlorinated pollutants.

3. Hydrodechlorination Catalysts

3.1. Synthesis of Catalysts for Hydrodechlorination. Active Phase and Support

The catalysts used in HDC consist of an active phase supported on a porous solid. The active phase is usually a noble metal such as Pd, Pt and Rh, due to their dechlorination and hydrogenation ability. Figure 2 shows the active phases used in HDC in the last 25 years. As can be seen, Pd and Pt are the most commonly studied metals. Mainly supported on activated carbon, they have yielded outstanding results. These metals have led to complete chloromethane conversion [1,23,28,29,31–33,35,37,39,49,52,56,75,85–87], high overall dechlorination [23,28,29,31–33,37,49,85,87], good stability [31–33,35,85] and high selectivity towards methane [1,23,29,32,33,35,37,47,85], C1+ light paraffins and olefins (C1+ referring to molecules with more than 1 carbon atom) [28,32,33,37,39,48–50,69,75] or even TCM (from the HDC of TTCM) [42,50,54–56,68,81–83]. Most of the HDC studies have been performed using catalysts with a 1–3 wt.% of active phase [1,19,24,28,30,47,50,54,55,57,59,61,65,69,73,80,86]. In general, within a given range of 0.5 to 4 wt.%, increasing the concentration of active phase increases the catalytic activity [23,54,88]. However, concentrations above 6 wt.%, may lead to metal sintering, hindering the

active phase–support interaction, lowering the accessible active centers and decreasing the activity [88]. In general, Pd has exhibited higher activity than Pt, due to its specific electronic structure [89], and to its commonly higher amount of electro-deficient (M^{n+}) species present in the surface of the catalysts [90]. Some metals, like Pd, have been demonstrated to have dual nature [Pd^0-Pd^{n+}], obtaining a better performance when the proportion of both species are similar Pd^0/Pd^{n+}~1 [89]. On the other hand, Pt, which mainly contains Pt^0 species, has shown higher hydrogenation ability than Pd. During the HDC of DCM with different metallic catalysts supported on activated carbon [31,36], Pt/C only generated methane and MCM, the former being the main product, with ca. 90% selectivity. On the contrary, with Pd/C, besides methane and MCM, ethane was also obtained [31,36]. Moreover, Pt/C showed much higher stability than Pd/C, which might also be related to its excellent hydrogenation ability [31,36]. In recent years, an increasing number of bimetallic systems have been reported in the literature, which combine the properties of both metals to obtain improved results [21,37,42,47,54,57–63,65,80,85,91–93]. In general, the use of bimetallic systems in HDC promotes higher chloromethane conversion and overall dechlorination, and better stability than the monometallic catalysts [59,61–63,65,73,85,92]. The synergistic effect observed has been related with the better active phase dispersion or its more favorable oxidation state [64,65,90]. Martin-Martinez et al. [85] supported Pd and Pt in different proportions on an activated carbon and compared the activity of these bimetallic systems in the HDC of DCM with some monometallic Pd/C and Pt/C catalysts. All the bimetallic catalysts showed better activity and dechlorination ability than the monometallic catalysts, and higher selectivity to the main product (CH_4). On the other hand, Karpiński et al. [55,59,81] also found that adding Au to a Pd/SiO_2 catalysts resulted in more stable systems; while Pd/SiO_2 suffered a 90% of deactivation after 60 h during the HDC of TTCM, a Pd-Au system with a 40 wt.% relative amount of Au decreased the deactivation to a 25%, and using only a 10 wt.% of Au resulted in high catalytic stability.

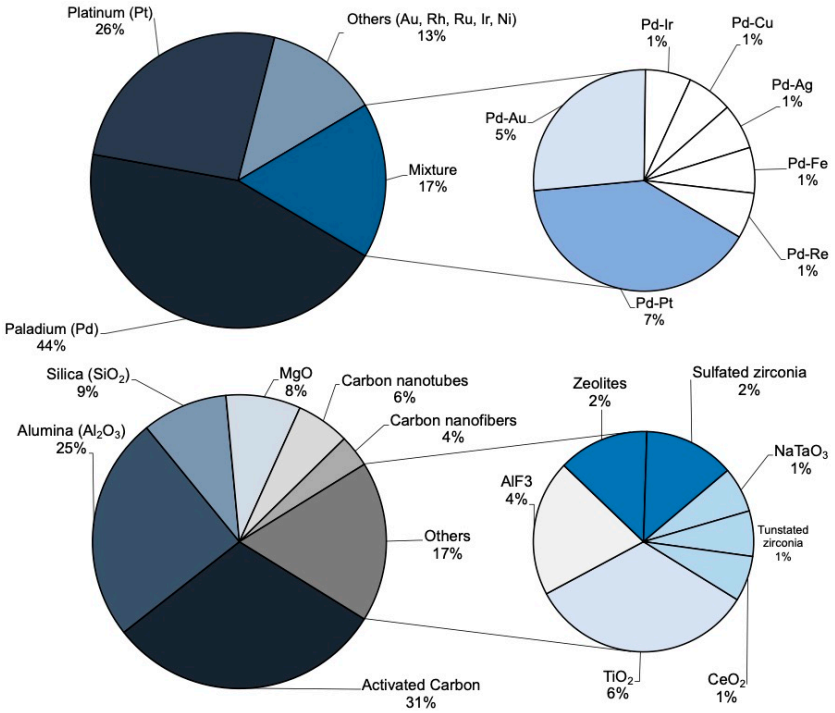

Figure 2. Active phase metals and support materials used in HDC of chloromethanes in the last 25 years.

The catalytic activity does not only depend on the active phase. The metal–support interaction is a key factor regarding the activity and selectivity [48,49]. Different porous materials with high surface area have been used as supports, allowing a good dispersion of the active phase [94].

As can be seen in Figure 2, activated carbon [1,23,28,29,31,33–39,47–49,61,68,80,85,89,95–97], alumina [19,24,30,40,44,51,54–57,65,66,68,86] and silica [59,68,87,92,98] have been the most commonly used supports for the HDC of chloromethanes in the last 25 years. N-doped supports have shown high hydrogen spillover, useful for the HDC of other chlorinated compounds (1,2-dichloroethane). As observed with Ni catalysts over N-doped porous carbon [99], this feature of the support may affect the selectivity [100–102].

The most widely used method for the synthesis of HDC catalysts is impregnation, consisting in the deposition of the active components on the support surface by means of their liquid solution [103]. Typical metal precursors are chloride or nitrate salts. Impregnation can be performed by incipient wetness (IWI) [32,48,104], where a volume of the active phase containing solution equal to the pore volume of the support is added, or by wet impregnation [105,106], where an excess of active solution is used. In addition to its technical simplicity, the IWI method has shown uniform distribution of the active phase, becoming the most commonly used method for the preparation of heterogeneous catalysts. Other procedures used as well, like precipitation or deposition–precipitation [107], do not ensure the control of the active phase particles' size and distribution. Direct redox methods are used to add another metal on the prepared catalyst [96,108]. On the other hand, for the synthesis of catalysts based on zeolites or resin materials, ionic exchange is the most suitable method, since active metals anchor on the support, replacing protons or other cations [109–112].

In all the cases, the catalysts need to be activated before their use in HDC by calcination and/or reduction treatments [52,113]. Reduction is usually performed under H_2 flow, using the appropriate temperature to allow the reduction of the active phase (typically between 250 and 400 °C) [1,30,92,114]. Other reducing agents, although less common, are hydrazine [115], formic acid [116] and $NaBH_4$ [117].

The methods and conditions used for the synthesis and activation of the catalysts will determine their properties, like metal particles size and oxidation state, as well as accessibility and distribution over the support.

3.2. Catalyst Properties and Their Effect on the Catalytic Activity

3.2.1. Metallic Particle Size and Dispersion

The smaller metallic particle size and better dispersion of the active centers have usually been related to a better overall catalytic activity for the HDC of different chlorinated hydrocarbons [11,31,47,48,50,57,60,81,88,90,91,118,119], though overly small particles have been suggested to have limited activity for some systems [88,120], since they may not be completely reduced before the reaction [88]. In contrast, most of the studies report an increase in activity per catalytic center, known as intrinsic activity or turnover frequency (TOF), when increasing the metal particle size, for the HDC of chloromethanes [21,23,24,32,49,121,122], indicating that the reaction is sensitive to the structure. Furthermore, particle size has proven to have a strong effect on the coordination of the metallic surface atoms. Nanoparticles that are smaller in size lead to higher proportions of edges and corners, which may act as active sites [120,123,124]. There is no consensus on the effect of metal particle size on the selectivity of HDC reactions. No effect was observed in some studies concerning the HDC of TTCM and TCM [66,122] as the selectivity was mainly influenced by other factors like metal oxidation state. However, in other studies with the same reactants, big metallic particles were found to promote oligomerization of reaction intermediates, leading to higher selectivities to C1+ hydrocarbons [35,51]. Higher metal dispersions probably lead to a higher concentration of H_2 in the vicinity of metallic active centers and higher spillover of H_2, thus favoring the reaction of adsorbed organochloride radicals with the surrounding H_2 and impeding the reaction with other adsorbed organochloride radicals. On the other hand, in a recent study, small metal particles were found to enhance selectivity to olefins during the HDC of TCM with Pd/C catalysts, probably due to the lower hydrogenation capacity of these smaller particles to produce the completely hydrogenated hydrocarbons [48]. A significant influence in metal particle size on selectivity was

found for other HDC reactions [51,125,126]. Regarding the stability, small particles were found to be prone to deactivation, mainly by HCl poisoning [52,55,120,123,124]. It is suggested that on the smaller particles (smaller than 2–3 nm), each surface metal atom is surrounded by a limited number of reactive atoms, increasing the adsorption energy of the reactants on the particle surface, and favoring the poisoning of the catalyst [120,123,124]. In contrast, smaller metal particles were also found to prevent oligomerization and coke formation during the HDC of chloromethanes, leading to more stable catalysts [31,35,48,85]. Smaller metallic particles with a more homogeneous size distribution, showing very little agglomeration and with a uniform distribution over the support, were found to contribute to the inhibition of the formation and stabilization of C1+ chlorocarbons at the active centers. Moreover, larger particles appear to favor metallic phase changes, like formation of Pd carbides (as was the case in the HDC of DCM [31]).

3.2.2. Oxidation State of the Active Centers

The oxidation state of the active centers has been revealed as critical in the catalyst performance. In general, the active centers present a dual nature, being constituted by zero-valent (M^0) and electro-deficient (M^{n+}) active centers. Both species have demonstrated their importance for the HDC [1,21,23,28,29,31–37,42,43,46,48,49,51,80,83,85,89,127–131]. M^{n+} species are usually originated by the interaction of metal particles with the support surface, as a consequence of the presence of different surface groups or those originated by the interaction with metal precursor during catalyst preparation. According to the mechanism showed in various studies [35,89,132], the use of acid solutions of Pd chloride for the preparation of Pd catalysts leads to the formation of tetrachloropalladic acid (H_2PdCl_4). The adsorption of H_2PdCl_4 on the support liberate protons. Furthermore, the interaction of these electrophilic protons with the neighboring electron-donating Pd^0 atoms, induces the formation of Pd^{n+} species, which are stabilized by the Cl^- remaining on the catalyst surface (Scheme 1).

$$Pd^0 + H^+ + Cl^- \rightarrow Pd^{n+} \cdots H^{(1-n)+} \cdots Cl^-$$

Scheme 1. Formation of the electro-deficient Pd sites [89].

The behavior of M^0 and M^{n+} species in the HDC reactions highly depends on the nature of metal and the reactant. While M^{n+} species were found to be more active for the HDC of chloromethanes with Pd, Rh and Ru, Pt^0 was found to be the main active center for the HDC of DCM and TCM [1,23,31,35,36,41,46,85]. The existence of an active center that is dual in nature was proposed in some studies for the liquid-phase HDC of TTCM to TCM [89] and gas-phase HDC of DCM [38] with Pd catalysts. The active site was proposed to be constituted by the association of the two species: electron-deficient palladium (Pd^{n+}) and metallic palladium (Pd^0). The highest TOF value was obtained for $Pd^{n+}/Pd^0 \sim 1$ [89]. On the other hand, the M^{n+} species enhances the diversity of non-chlorinated hydrocarbons [31,46], but usually leads to the deactivation of the catalysts through the promotion of oligomerization reactions and further irreversible chemisorption on active centers, as well as the irreversible generation of metal carbides [29,31,48]. Moreover, Pd^{n+} species were found to be prone to deactivation by the irreversible non-dissociative adsorption of the chloromethanes [37,127]. Contrarily, M^0 favors the stability of the catalyst [1,29,31,35,120]. The proportion of both species mainly depends on the activation (reduction) step of the catalysts and the interaction of metal particles with the support, as stated above. Nevertheless, M^{n+} happens to be also formed during the reaction [29,31,35,41], proving their stability in the presence of hydrogen, even after careful reduction at about 450 °C.

3.2.3. Surface Acidity

Surface acidity also plays an important role in the final activity. First, surface acidity usually contributes to increases in the electro-deficiency of metallic species, with the consequences exposed above [48,49,53,133]. Attending to the selectivity, acidity seems to favor the hydrogenation reactions, contributing to increases in the selectivity to methane, to the detriment of other olefinic and paraffinic

hydrocarbons in the HDC of TCM [48,53,134], and contributing to increases in the selectivity to complete hydrogenated hydrocarbons in the selective HDC of TTCM to TCM [81,83]. Similar results were obtained in the HDC of other compounds. The acidity increase in the catalysts during the HDC of CCl_2F_2 with Pd/Mg–Al hydrotalcites and Pd/MgO, enhanced the yield of CH_2F_2 [135]. On the other hand, acidity has a remarkable role in the deactivation of hydrodechlorination catalysts. The presence of acid centers in the support could accelerate the deactivation of the catalyst through the formation of carbonaceous deposits (coke) [40,41,48,51,53,60,66,136–138]. The deactivation mechanism is explained in Section 6.2. For these reasons, basic catalysts have been identified as more interesting for HDC purposes by many authors [48,53,95]. Finally, surface acidity also interferes in the metal particle size, affecting the final catalytic activity, selectivity and stability, as stated in Section 3.2.1. The mechanism depends on the type of acid sites present in the catalyst surface. It is well known that surface acid sites may promote the formation of metal particles of small sizes, since they increase the hydrophilic character of the support, favoring the diffusion of the metal precursor [32,133,134]. However, strong acid sites were found to provoke the reverse effect. In a recent work devoted to the HDC of TCM [49] with Pd catalysts supported on activated carbons synthesized using different activation agents, the presence of C–O–P surface groups (due to the remaining phosphorus from the activating agent) providing very strong acid sites led to Pd particles of greater sizes (13–15 nm) than those obtained with other carbonaceous supports (2–5 nm). This was attributed by other authors to different phenomena, like the enhancement of support degasification under the reductive treatment or the hindering of anchorage of the Pd precursor [122]. The formation of these C–O–P surface groups and their contribution to the formation of strong acid sites was previously reported by other authors [139–141].

3.2.4. Structure of the Support

Metal–support interactions are crucial for the catalyst performance, and the morphology of the support necessarily influences the orientation of the metal particles, exposing their terraces, edges or corners. As was noted before, activated carbon is the most frequently selected material used as catalytic support, due to its excellent adsorption properties, surface chemistry and low cost. Moreover, the lower acidity of the surface when compared to other supports like silica, alumina or zeolites leads to more stable catalysts [41]. The main mechanism of surface acidity for the deactivation of the catalysts is the promotion of carbon deposition [70,81,142]. Nevertheless, catalysts based on activated carbon may also suffer from severe deactivation. Amorim et al. [97], compared the catalytic stability of Pd catalysts over three different types of carbonaceous supports, activated carbon, graphite and graphitic carbon nanofiber (GNF), during the HDC of chlorobenzene, concluding that structured GNF led to the most stable catalyst, while amorphous activated carbon showed the highest deactivation. Besides, the use of structured carbon nanotubes (CNT) and nanofibers (CNF) have demonstrated superior catalytic activity, favoring the dispersion of the active phase [81,143,144].

3.2.5. Functional Groups and Doping

Carbon-based supports, such as activated carbon, carbon nanotubes and nanofibers, graphene, etc. [145], may usually contain oxygenated (hydroxyl, carbonyl, carboxyl, acyl, alkoxy, etc.), nitrogenated (amino, nitro, nitrile, azo, etc.), sulfurated (thiol, sulfide, sulfo, etc.) or even halogenated groups [31,35,48,145].

The introduction of functional groups or heteroatoms in the catalysts can be performed by different methods, including: (i) noncovalent functionalization, adsorption or wrapping of functional molecules on the material [146]; (ii) covalent functionalization, chemical treatment, such as oxidation using carboxylic, nitric or sulfuric acid [137,146], or under microwave conditions through the 1,3-dipolar cycloaddition reaction [147]; (iii) thermal treatment, heating under inert environment for removal of some functional groups [148]; (iv) reaction with an heteroatom-containing reagent [149]; or (v) pyrolysis with precursors containing the desired heteroatoms [95,149,150].

The presence of functional groups or heteroatoms on the catalysts' surface might strongly affect the properties of the catalysts and their catalytic activity. Oxygenated groups like -COOH contribute to the acidity of the catalyst, whereas amino groups may provide basicity or act as Lewis acids. Several studies correlate the high concentration of oxygenated or acid groups with the higher proportion of M^{n+} [48,53,151–156], which may increase the activity of the catalysts, but also promote their deactivation. The presence of different surface functional groups may also affect the selectivity of the process. A higher concentration of surface oxygenated groups has been correlated with a higher hydrogenation extent of hydrocarbons produced by the HDC of chloromethanes [1,31,34,35,48]. Particularly, C=O groups appear to show a high hydrogenation ability. As a consequence, recent studies have reported higher selectivities to C1+ paraffins with catalysts containing a higher proportion of C=O groups, since these groups favor the hydrogenation of olefinic intermediates into paraffins [34,48]. Besides, some nitrogenated groups have been proven to enhance the interaction of active centers with the support, avoiding the sintering of the active centers and leading to the uniform dispersion of the metallic particles, improving catalytic activity [147]. Doping with heteroatoms like N, B, P, S, etc. may also alter the physico-chemical properties of the catalysts [145]. Among them, N-doping has received increasing attention in recent years. Due to the much stronger metal–support interaction provided, N-doped catalysts have shown excellent activity improvement compared to the undoped catalysts [95,99,145,150].

4. Reaction Systems and Operation Conditions

In this chapter, the influence of operating conditions such as temperature, pressure, space-time, H_2/CM molar ratio and the reaction systems used, in the HDC of chloromethanes, is analyzed. Table A1 (in Appendix A) summarizes the main results obtained at different operation conditions.

4.1. Reaction Systems

One of the advantages of HDC is that it can be operated in both continuous and discontinuous mode. The reaction system used for HDC mainly depends on the physical state of the inlet reactant. Among the four existing chloromethanes, MCM is the only gas. The other are liquids at standard conditions but can be used in gas phase if pressurized or vaporized [19,57,67,90] before being fed into the reactor. Thus, most of the HDC studies have been performed in the gas phase, by means of a continuous flow reaction system [1,31,34,35,57,59,60,66,68,85,87,91,134], using an inert tubular quartz or glass fixed bed reactor [1,11,19,30,31,34,35,47,50,53,54,59,65,80,81,85,87,91,97,134,157], usually integrated in an automatic system with control of the operating conditions [1,19,27,31,34,35,40,50,51,53,59,65,66,80,85,87,90]. For the liquid-phase HDC of TTCM, a discontinuous flow reaction system with a semi-batch mode reactor [82,144,158,159], and a high pressure flow reaction system in which a mixture of TTCM and H_2 is fed [56,61], have also been employed. Similar initial conversions of TTCM (>90%) and selectivities to the main product (TCM, 50–80%) were obtained when using the gas-phase reaction system [54,66,67,138] and the liquid-phase system [54,56,66,67,138]. On the other hand, although the semi-batch mode reactor showed lower and unstable conversion of TTCM [82,89], the selectivity to TCM with this system reached 90–100% [82,89].

4.2. Effects of Operating Conditions

The effectiveness of the process does not only depend on the reaction system, but on the operating conditions used, as will be illustrated in this section. In most of the studies analyzed in this review, atmospheric pressure and temperatures between 100 and 350 °C were used, even though some studies have tested more severe conditions.

4.2.1. Reaction Temperature

Reaction temperature is a key variable in HDC. Thermal stability of chloromethanes diminishes when increasing the number of chlorine atoms in the molecule, and this has been experimentally

stablished at 875, 780, 675 and 635 °C for MCM, DCM, TCM and TTCM, respectively [17,18]. Since one of the advantages of HDC is that can be carried out at moderate conditions, temperatures of up to 450 °C have been used in the HDC of CMs. The effect of the reaction temperature has been analyzed in several articles (Figure 3), achieving higher conversions when using higher temperatures [1,28,35,37,38,42,50,69,85,87], since higher temperatures increase the reaction rate, as occurs in most catalytic processes. In particular, employing Pd/C (space-time of 1.8 kg·h·mol^{-1}), the conversion of MCM increased from ca. 10% to 35% when increasing the temperature by 75 °C (from 175 to 250 °C) [1,28]. For DCM, which has usually been studied in gas phase, 100% conversion has been reported at temperatures of 250 °C or higher (250–400 °C), employing different catalysts, such as Rh/C and Pd/zeolite [1,32,33]. Lower temperatures (125 °C or higher) are needed for achieving complete conversion of TCM in gas phase with Pd based catalysts [1,23,27,28,32,33,35,49]. Even lower temperatures (90–150 °C) are enough to reach 100% conversion of TTCM in gas phase HDC [51–56,70,76,80,138]. In the liquid phase HDC of TTCM, however, higher temperature (300 °C) and pressure (30–70 bar) would be required [27,57,72]. In general, Pt/Al_2O_3 catalysts have been preferably employed for achieving complete conversion of TTCM in HDC reactions [27,51,54–57]. TOF also increases with temperature [1,98]. However, overheating the system may promote the sintering of the active phase, worsening the catalytic activity [44]. Besides, using higher temperatures entails higher operational costs.

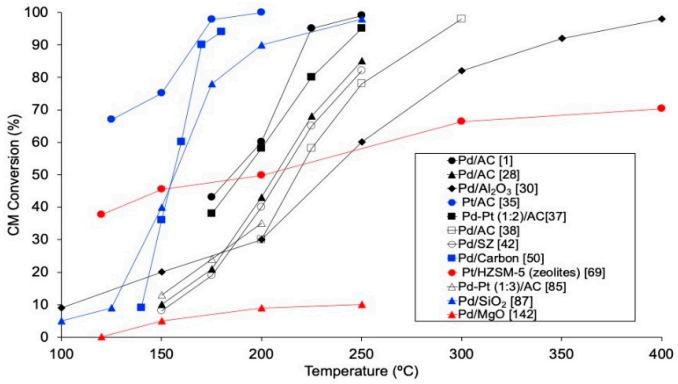

Figure 3. Evolution of the conversion of chloromethanes with temperature in the HDC of DCM (black), TCM (blue) and TTCM (red) in the literature.

Increasing the reaction temperature may also modify the selectivity of the process, enhancing the dechlorination ability of the catalysts [1,28,41,42,50,51,69,76,85,160]. Thus, the reaction temperature may be increased in order to increase the selectivity to target non-chlorinated products, such as CH_4 [35,41,50], C_1+ paraffins [32,36,39,49,69], or even light olefins, even though higher temperatures (250–400 °C) might be used for this purpose [33,48]. On the other hand, depending on the structure, the Si/Al proportion or the acid to basic ratio, the selectivity trend of zeolitic catalysts may completely change. Fasi et al. [69] observed a higher selectivity to the main product (C_2H_6) when increasing the reaction temperature from 120 °C to 400 °C in the HDC of TTCM with Pd/HY catalyst.

4.2.2. Pressure

Most of the studies are performed at atmospheric pressure, enough for achieving high HDC efficiencies. Yet, a few gas phase HDC studies have been done at higher working pressure, in order to analyze its effect over the process [40,51,56,57,82,83,89], or using a vacuum, a situation in which the dechlorination seems not to be favored [51,57]. When increasing the pressure from 25 to 100 bar, DCM conversion increases from 65% to 95% during its HDC with NiO-MoO_3/Al_2O_3 [40]. A lower range (1–10 bar) was tested for the HDC of TTCM with Pt/Al_2O_3 [56], finding that increasing the pressure promoted the dissociative adsorption of hydrogen on the catalysts, enhancing the

selectivity to chlorinated TCM. Nevertheless, above 7 bar (identified as the optimum pressure for the reaction), due to the relatively hydrogen-deficient environment (compared with the dissociatively adsorbed TTCM), oligomerization of the adsorbed TTCM into C_2Cl_4 precipitated catalyst deactivation. In liquid phase HDC of TTCM, to obtain better catalytic activity, high-pressure conditions are usually needed [27,72,82,83,89,114]. Increasing the working pressure from 30 to 70 bars, the conversion of TTCM may exceed 90%, maintaining high selectivities to the desired products (i.e., C_2H_6 or TCM) [27,72,82,83,89].

4.2.3. Space-Time

The space-time can be defined as the relation between the mass of catalyst used and the molar flow of chloromethane treated (Equation (1)):

$$\tau\left(\text{kg·h·mol}^{-1}\right) = \frac{\omega_{cat}\ (\text{kg})}{F_{CM_0}\left(\text{mol·h}^{-1}\right)} \quad (1)$$

The space-time used in the HDC studies analyzed in the current revision ranges between 0.08 [28] and 4 [35] kg·h·mol^{-1}. Due to the longer contact time between the reactants and the catalyst surface (i.e., between the chloromethane and the active phase), increasing the space-time favors the conversion of chloromethanes [1,19,35,36,39,76,122,142], irrespective of the catalyst or reaction temperature used. In general, this effect is more substantial when operating at lower space-times [23,35,69]. In the HDC of TTCM, most of the studies are performed in a discontinuous system. Thus, instead of space-time, the effect of the mass of catalyst is studied [68,86,122,142], finding that the activity always increases when increasing the mass of catalyst from 50 to 300 mg. As an example, the conversion of MCM over Pd/C at 250 °C increased from 5% to 35% when increasing the space-time from 0.1 to 1.8 kg·h·mol^{-1} [1]. With DCM, complete conversion (from 20%) was achieved with Rh/C at 250 °C when increasing the space-time from 0.1 to 1.8 kg·h·mol^{-1} [1,35,39], and with Pd/Al_2O_3 at 300 °C when increasing the contact time from 1 to 10 s (from 40%) [20]. On the other hand, a decrease in space-velocity (the inverse of space-time) from 200 to 25 cm^3·min^{-1}·g^{-1} led to an increase in DCM conversion from 20% to 75% at 200 °C using Ir/TiO_2 [20]. Complete conversion was obtained for TCM (from 60%) when increasing the space-time from 0.1 to 1.8 kg·h·mol^{-1} at 175 °C using Pd/C [1], and for TTCM when increasing contact time from 1.5 s to 6 s using Pt/Al_2O_3 (from 78%) [76] or decreasing space-velocity from 75,000 L·kg^{-1}·h^{-1} to 9000 L·kg^{-1}·h^{-1} with Pt/MgO (from 50%) [70].

Although at lower extents, the space-time may also affect the selectivity of the process, a higher contact time between the reactants and the catalytic surface may extend the evolution of the reaction, obtaining secondary products (saturated hydrocarbons like C_2H_6, C_3H_8 and C_4H_{10}) from unsaturated intermediates (C_2H_4, C_3H_6 and C_4H_8) [1]. When the target product is a chlorinated compound (MCM, DCM, TCM), increasing the space-velocity has served as a good strategy for increasing its selectivity [45,47].

4.2.4. Ratio H_2/Chloromethane

In addition to being a key condition for the economy of the process, the concentration of H_2 used is critical, since it may affect the catalytic activity and stability, and may favor the production of different compounds. The influence of the molar ratio H_2/chloromethane has been investigated in several studies [30,32,39,48,55,56,70,71], observing that increasing the concentration of H_2 entails a higher conversion of the chloromethane (Figure 4). Nevertheless, this effect is not equally intense for low and high ranges of this variable. De Pedro et al. [39] studied the HDC of DCM with Pd/C, finding a remarkable development of the DCM conversion when increasing H_2/DCM up to 100, while increasing this variable from 100 to 400 showed only a minor improvement of DCM conversion. In the same reaction at 250 °C, increasing the molar ratio of H_2/DCM from 3 to 10 led to a DCM conversion increase from 45% to 60% [30], while an increase from 40 to 400 was needed for an additional increment of

DCM conversion to 80% [39]. Complete TCM conversion might be obtained (from 44%) with the same catalyst at 125 °C if the molar ratio of H_2/TCM was increased from 50 to 100 [48,49], and in the HDC of TTCM, increasing the molar ratio of H_2/TTCM from 5 to 15 caused an increase in TTCM from 78% to 95% [70]. Regarding the selectivity, a higher concentration of H_2 helps the hydrogenation of the chlorinated reactant [48,56,76]. This might be used to favor the production of non-chlorinated products (in the HDC of TTCM with Pt catalysts, a small increase in H_2/TTCM molar ratio from 5 to 10 led to a remarkable increase in selectivity to CH_4, C_2H_6 and C_3H_8 from 57% to 84% [76]) or the production of TCM from TTCM (selectivity to TCM increased from 69% to 74% when increasing the H_2/TTCM ratio from 9 to 15 [56]). In addition, the proportion of paraffinic to olefinic products obtained may be strongly affected by the ratio H_2/CM. Olefins have been identified as intermediate products in the HDC, which may further incorporate additional hydrogen to form the corresponding paraffinic hydrocarbons [1]. Thus, decreasing the proportion of H_2 used would favor the production of light olefins [48].

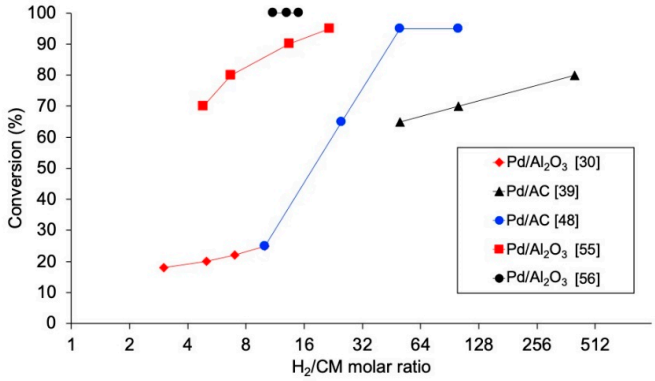

Figure 4. Evolution of the conversion of chloromethanes with molar ratio H_2/CM in the HDC of DCM (black), TCM (blue) and TTCM (red) in the literature.

5. Mechanism and Kinetics

A few theoretical and experimental studies in the literature have tried to clarify the mechanism of HDC reactions and define the kinetics of the process. Most of them are related to the HDC of chloroaromatic compounds. Among the aliphatic chloromethanes considered in the current review, the kinetics of the HDC of TTCM has been the most widely studied [27,52–55,58,60,65,72,82,161,162], mainly using Pd-based catalysts. In this section, we will summarize the main conclusions regarding the HDC of chloromethanes.

5.1. Mechanism Studies

There is consensus in that the first step for the HDC of chloromethanes is the dissociative adsorption of the chlorinated compound on the catalyst surface [27,47,58,161,162], which proceeds via the breaking of a C-Cl bond (thermodynamically more favorable than breaking a C-H bond) [72,161]. The dissociation of the first C-Cl bond has been identified as the rate-controlling step in the HDC of the four chloromethanes with a Pd/C catalyst. Chen et al. [161] studied the reaction experimentally, by isotope exchange experiments, and theoretically, by density functional theory (DFT) calculations on Pd(110). They found that the activation energy needed for the dissociation of the first C-Cl bond decreased as the number of chlorine atoms increased in the molecule, and explained it in view of the geometry of the transition state formed. The distance between the carbon atom and the Pd surface increased with the number of chlorine atoms. For TTCM, the geometry of the transition state was closer to the configuration adopted during a molecular adsorption (the initial state), while for DCM, it was closer to the final state. After the first dissociation, the resulting chlorinated fragments might subsequently be adsorbed on the Pd surface, by consecutive C-Cl scissions. Hence, the reactivity of

chloromethanes in the HDC was theoretically proven to decrease in the following order: TTCM > TCM > DCM > MCM. Similar mechanisms were proposed in other experimental studies [27,38,52,72]. De Pedro et al. [38] studied the reaction pathway of the HDC of DCM over Pd/C, proposing the mechanism shown at Scheme 2 (solid arrows): First, a DCM molecule was dissociatively adsorbed on the Pd surface, producing a chlorocarbene radical ($^{\bullet}CH_2Cl$); then, this radical hydrogenates to MCM, or dissociates generating a new carbine intermediate ($^{\bullet\bullet}CH_2$); finally, this intermediate could evolve to methane by hydrogenation, or dimerize to form a bigger radical ($^{\bullet\bullet}C_2H_4$) from which ethylene and ethane should be produced. DFT calculations [127] suggested that, in the first step, a DCM molecule could also completely dechlorinate to form a $^{\bullet\bullet}CH_2$ radical in a single step (Scheme 2, dotted arrow), opening parallel pathways for the production of methane and MCM. The existence of these parallel routes has also been proposed in experimental studies for other chloromethanes [1,52,72]. As shown at Scheme 3, during the HDC of TTCM with a Pd/C catalyst, first, a TTCM molecule is dissociatively adsorbed on the catalyst surface, producing a Cl-CCl_3, from which three parallel routes are described [72]: (i) interaction with adsorbed H_2 to form the primary product TCM, and subsequent similar steps to produce the secondary products DCM and MCM; (ii) interaction of two neighbor Cl-CCl_3 to form C_2Cl_6, which is an intermediate of the primary product C_2Cl_4; and (iii) substitution of the four Cl atoms by H atoms to form the primary product CH_4. This third route has been proposed to occur in a single step [72] or as a consecutive substitution process occurring on the same active center [163,164]. Other authors have also described additional routes for the production of C2-C4 hydrocarbons by oligomerization of intermediates adsorbed on neighboring active centers [1,38,52]. Besides, depending on the catalyst used, saturated C2-C4 hydrocarbons, such as ethane and propane, have been found to be secondary products generated from their unsaturated homologues (ethylene and propylene) [1].

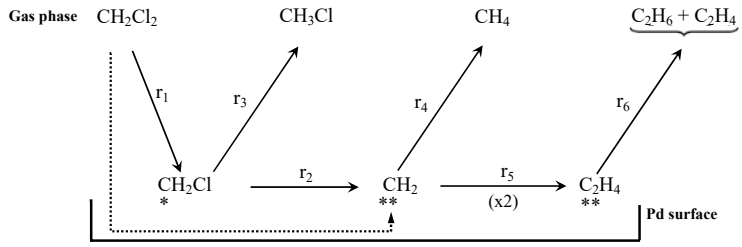

Scheme 2. Reaction scheme for the HDC of DCM proposed in ref. [38] (solid arrows) and correction proposed from DFT calculations in ref. [127] (dotted arrow). Reprinted with permission from ref. [127].

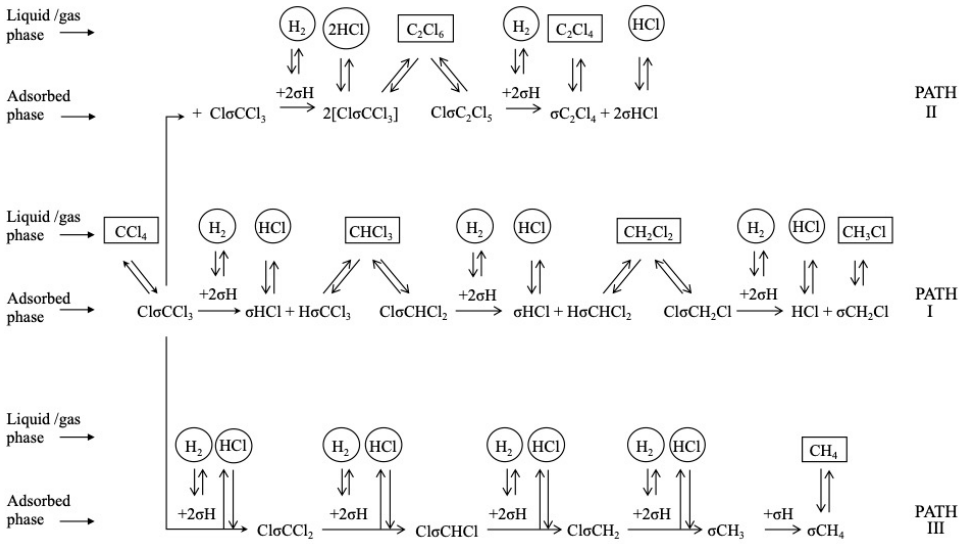

Scheme 3. Reaction mechanism for the HDC of TTCM. Reprinted with permission from ref. [72].

5.2. Kinetics Studies

According to the mechanisms proposed, two main kinetic models have been evaluated for the HDC of chloromethanes: (i) the pseudo-first-order kinetic, with rate linear dependence on only the concentration of the chloromethane, since H_2 is usually fed in excess; and (ii) the Langmuir–Hinshelwood (LH) model, which considers the dissociative adsorption of both reactants (chloromethane and H_2) on the catalytic surface, their reaction via hydrogenolisis, and the desorption of products.

Some studies [38,43] have adjusted the experimental HDC results to a pseudo-first order rate with relative success, using Equation (2) (Table 1), coming from the application of the mass balance in a catalytic fixed-bed reactor [38], where τ is the space time (in kg h mol^{-1}), W is the catalyst weight (kg), F_{CM} is the inlet molar flow of chloromethane (mol h^{-1}), k' is the lumped kinetic constant (h^{-1}), which includes the dependence on the hydrogen concentration, used in large excess, C_{CM_0} is the inlet concentration of chloromethane (mol L^{-1}) and X_{CM} is the conversion of chloromethane. This model was successfully applied by López et al. [19] to describe the reaction rate for the HDC of DCM with Pd/Al_2O_3. Nevertheless, when mixtures of DCM with other chlorinated compounds (tetrachloroethylene, chlorobenzene, 1,2-dichlorobenzene) were studied, the kinetic was better represented by a LH model, due to the important inhibition effects shown by the mixtures [19].

Table 1. Kinetic equations obtained from the application of the pseudo-first order or the LH models.

Kinetic Model	Kinetic Expression	Equation	Ref.
Pseudo-first order, catalytic fixed-bed reactor	$\tau = \frac{W}{F_{CM}} = \frac{1}{k' \cdot C_{CM_0}} \cdot \ln(1 - X_{CM})^{-1}$	(2)	[38]
LH model	$r = \frac{k'[R-Cl]}{1+K' \frac{[HCl]}{[H_2]^{0.5}}}$	(3)	[161]
LH model with DCM adsorption control, catalytic fixed-bed reactor	$\frac{dC_{DCM}}{d\tau} = C_{DCM_0} \cdot \left(-\frac{k_1 \cdot C_{DCM}}{1+K \cdot (C_{DCM_0} - C_{DCM}}\right)$	(4)	[38]
	$\frac{dC_{CH_3Cl}}{d\tau} = C_{DCM_0} \cdot \left(-\frac{k_{CH_3Cl} \cdot C_{DCM}}{1+K \cdot (C_{DCM_0} - C_{DCM}}\right)$	(5)	
	$\frac{dC_{CH_4}}{d\tau} = C_{DCM_0} \cdot \left(-\frac{k_{CH_4} \cdot C_{DCM}}{1+K \cdot (C_{DCM_0} - C_{DCM}}\right)$	(6)	
	$\frac{dC_{C_2H_6+C_2H_4}}{d\tau} = C_{DCM_0} \cdot \left(-\frac{k_{C_2} \cdot C_{DCM}}{1+K \cdot (C_{DCM_0} - C_{DCM}}\right)$	(7)	
LH model with adsorption control, catalytic fixed-bed reactor	$\frac{dX_{CM}}{d\tau} = \frac{k_{ads} \cdot [CM]}{1+K_S \cdot [P]}$	(8)	[43]
LH model with chemical reaction control, catalytic fixed-bed reactor	$\frac{dX_{CM}}{d\tau} = \frac{k_r \cdot [CM]}{1+K_{ads} \cdot [CM] + K'_{des} \cdot [P]}$	(9)	
LH model with desorption control, catalytic fixed-bed reactor	$\frac{dX_{CM}}{d\tau} = \frac{k_{des} \cdot [CM]}{1+K_Z \cdot [CM]}$	(10)	

In general, the studies that considered both models, pseudo-first order and LH, have concluded that LH better describes the process. Chen et al. [161] observed that the reaction rate for the HDC of chloromethanes could be described by a LH model using Equation (3) (Table 1), where k' and K' are lumped kinetic and thermodynamic constants, only dependent on the reaction temperature. By comparing the relative turnover rates obtained by theoretical prediction and experimental data, they found the highest difference during the HDC of TTCM, and attributed it to the significant deactivation suffered by Pd/C during the reaction, not observed for TCM, DCM, or MCM. De Pedro et al. [38] also employed a LH model to describe the HDC of DCM with Pd/C. By accepting the adsorption of DCM as the controlling step (Equations (4)–(7), Table 1), the LH model successfully illustrated the conversion of DCM and the yield of the major products obtained. Álvarez-Montero et al. [43] studied the HDC of DCM and TCM with four metallic catalysts: Pd/C, Pt/C,

Ru/C and Rh/C. The authors evaluated the LH model with adsorption, chemical reaction, or desorption control. The kinetic equations from the application of the LH model in a catalytic fixed-bed reactor are shown in Table 1 (Equations (8)–(10), where k_{ads}, k_r, and k_{des} (in $NL \cdot kg^{-1} \cdot h^{-1}$) are the kinetic constants of adsorption, chemical reaction, or desorption control, respectively; K_S and K_Z (in $NL \cdot mol^{-1}$) are lumped equilibrium constants of adsorption and desorption control, respectively; K_{ads} (in $NL \cdot mol^{-1}$) is the DCM or TCM adsorption equilibrium constant of chemical reaction control; and K'_{des} (in $NL \cdot mol^{-1}$) is the product desorption equilibrium constant of chemical reaction control. This model successfully predicted the reaction rate-controlling step for the HDC of DCM and TCM. With the Pd and Pt catalysts, the LH model with reactant adsorption as the rate-controlling step adequately described the HDC, according with the results reported by other authors [38]. With the Rh and Ru catalysts, with lower hydrogenolysis−hydrogenation ability, chemical reaction was identified as the rate-controlling step in the HDC of DCM, while desorption of the reaction products was identified as the rate-controlling step in the HDC of TCM. This also explained the severe deactivation observed for these catalysts, due to the formation of oligomeric coke-like deposits.

5.3. Activation Energy for the HDC of Chloromethanes

The activation energies (E_a) for the HDC of chloromethanes have been calculated by different techniques in the literature, namely the Arrhenius plots of the initial reaction rates at different reaction temperatures [1,11,19,24,43,53,60,65,161,165], using the kinetic constants obtained from the application of the LH model assuming adsorption, reaction or desorption as the rate-limiting step [38,43,47], or by DFT calculations [26,161]. The values of E_a reported in the literature for the HDC of chloromethanes are presented in Table 2. In general, the E_a decreases as the number of chlorine atoms increases, due to the higher reactivity of the molecule.

Table 2. Activation energies for the HDC of chloromethanes.

	Catalyst	Method	E_a ($kJ \cdot mol^{-1}$)	Ref.
MCM	5% Pd/C	DFT	62.0	[161]
	5% Pd/C	Arrhenius	64.0	[161]
	-	Arrhenius	184.5 *	[165]
DCM	5% Pd/C	DFT	56.0	[161]
	5% Pd/C	Arrhenius	58.0	[161]
	1% Pd/C		50.9	[1]
	1% Pd/C		50.0	[43]
	0.5% Pd/C		52.3	[38]
	1% Pt/C		52.5	[1]
	1% Pt/C		49.0	[43]
	1% Rh/C		50.3	[1]
	1% Rh/C		39.0	[43]
	1% Ru/C		44.4	[1]
	1% Ru/C		64.0	[43]
	0.3% Pd/γ-Al_2O_3		130.2	[24]
	0.4% Pd/γ-Al_2O_3		114.7	[24]
	0.6% Pd/γ-Al_2O_3		92.5	[24]
	0.3% Pd/TiO_2		130.5	[24]
	0.4% Pd/TiO_2		129.3	[24]
	0.7% Pd/TiO_2		97.5	[24]
	-		237.6 *	[165]

Table 2. *Cont.*

	Catalyst	Method	E_a (kJ·mol^{-1})	Ref.
TCM	5% Pd/C	DFT	46.0	[161]
	5% Pd/C	Arrhenius	54.0	[161]
	1% Pd/C		32.4	[1]
	1% Pd/C		52.0	[43]
	1% Pt/C		32.4	[1]
	1% Pt/C		29.0	[43]
	1% Rh/C		17.1	[1]
	1% Ru/C		41.4	[1]
	-		243.5 *	[165]
	Pt/K6 Pd/K6 PtPd/K6(30) PtPd/K6(40) PtPd/K6(50) PtPd/SiC@K6(40) PtPd/SiC	Akaike's Information Criteria	18–60	[47]
TTCM	5% Pd/C	DFT	40.0	[161]
	5% Pd/C	Arrhenius	48.0	[161]
	-		256.5 *	[165]
	3% Pd/MgF_2-SolGel		38.3	[53]
	3% Pd/MgF_2-Carb		42.1	[53]
	3% Pd/MgO-SolGel		56.7	[53]
	3% Pd/MgO-Carb		48.5	[53]
	1% Pd/MgF_2-Carb		46.3	[53]
	1% Pd/MgO-Carb		65.0	[53]
	1.5% Pt/Al_2O_3		57.7	[55]
	1.5% Pt/SiO_2		53.8	[55]
	2.8% Pd/Sibunit carbon		51.9	[60]
	6.2% Pd60-Au40/Sibunit carbon		59.9	[60]
	1% Pt/Al_2O_3		56.0	[65]
	1% Pt95-Au5/Al_2O_3		22.9	[65]
	1.4% Pt70-Au30/Al_2O_3		26.4	[65]

* Calculated and scaled at 973.15 K< >700 °C.

Chen et al. [161] found that the E_a was linearly related to the energy of dissociation of the first C−Cl bond (identified as the rate-determining step). They calculated the E_a for the HDC of the four chloromethanes by DFT calculations and compared them with the values obtained by Arrhenius. Even though there is a small difference among the values calculated, they found a good agreement between both methods. The values calculated by Arrhenius applying the LH model also seem to differ slightly, which may be attributed to the better approximation obtained when considering the rate limiting step in the equation.

6. Catalysts Stability and Deactivation

6.1. Stable Catalysts in the HDC of Chloromethanes

As reported in previous sections, there exist several catalysts capable of providing high conversions of chloromethanes. However, stability is another important factor for measuring the feasibility of the catalysts for industrial applications. Though most of reported HDC catalysts show a significant deactivation after a few hours of operation, some catalysts can be found showing significant stability during the HDC of chloromethanes. Several studies have demonstrated that Pt-based catalysts could perform with outstanding stability during the HDC of DCM and TCM with moderate reaction conditions [1,21,31,35,36,42]. In general, Pt shows better stability when compared to other noble metals like Pd, Rh and Ru, even though Pd and Rh usually give rise to higher conversions [1,29,31,36]. In the

HDC of DCM [35], a Pt/C catalyst provided ca. 55% stable conversion of DCM during more than 26 days under continuous operation at 250 °C (Figure 5). This catalyst showed a potential resistance to deactivation, attributed to the re-dispersion of the Pt particles during the HDC, making it feasible for industrial applications. The addition of Pt to a Pd catalyst allowed the increasing of its stability in the HDC of chloromethanes, maintaining high conversions [21,42,85]. Bedia et al. [42], reported a Pt-Pd catalyst supported on sulfated zirconia which maintained nearly 80% of DCM conversion for 80 h.

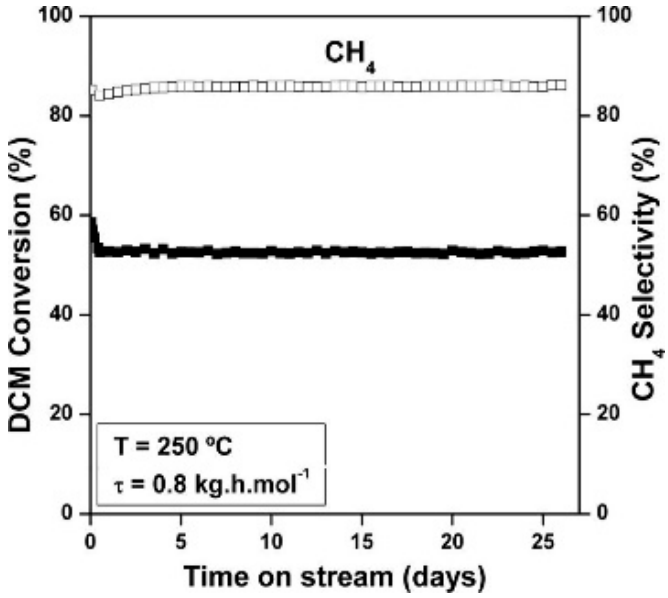

Figure 5. Evolution of DCM conversion and selectivity to CH_4 with time on stream for a Pt/C catalyst at 250 °C and 0.8 kg h mol^{-1}. Reprinted with permission from ref. [35].

Since the deactivation is a common problem surrounding the catalysts, the causes of deactivation and the regeneration of the catalysts used in the HDC reactions will be discussed deeply in the next sections.

6.2. Catalysts Deactivation in the HDC of Chloromethanes

Despite providing high conversions of chloromethanes, most of the catalysts reported in the literature suffer a serious deactivation, which may even alter the mechanism and kinetics of the process [25,29,31,34,44,48,73,97,166–172]. The deactivation of catalysts in the HDC has been attributed to different origins, including poisoning, sintering of the active centers, and formation of deposits blocking the porous structure, but only a few of these studies refer to the HDC of chloromethanes.

6.2.1. Poisoning of the Catalysts

The main subproduct formed during the HDC of organochlorinated compounds is HCl (g). This HCl or other chlorinated byproducts might poison the metallic phase of the catalyst by adsorption, giving rise to changes in their electronic structure and/or the nature of their surface groups [27,29–31,34,48,67,167,168,173–182]. In any HDC process, HCl may migrate inside the catalyst, clouding the metallic particles, and poisoning the catalytic active phase [90,183]. Moreover, the loss of active phase may even occur due to the formation of surface metallic halides (chlorides) [11,30,80,184]. The local excess of HCl around the catalyst can be reduced by operating under continuous conditions in a fix-bed reactor [166], or selecting the adequate catalytic components [30,64,183], since the metal–support interactions determine the active phase particle size, which, as explained in Section 3.2.1, has an important influence on poisoning by HCl, and the molecular adsorption, including HCl.

Other common poisoning agents identified in some recent HDC studies are the chloromethane reactants themselves or other chlorinated species produced during the HDC, which can be absorbed in the palladium metallic species leading to the formation of palladium carbide (PdC_x), inactivating the active centers [29,31,48,80]. Pd^0, present after the activation of the catalyst by reduction, may be transformed into Pd^{n+} by interaction with the HCl (Scheme 1) [29]. This causes a dual effect, first, hindering the dissociation of H_2, needed for the HDC, and second, contributing to the chemisorption and incorporation of carbon atoms into the metal lattice, leading to the formation of PdC_x [29,31]. The presence of this new phase poisoning the catalyst has been verified by XPS, XRD, or electronic microscopy [29,31].

The inappropriate structure of the active phase may also accelerate the poisoning of the catalysts. Xu et al. [26] investigated the sensitivity of HDC of TCM depending on the structure of Pd. They performed a DFT study on Pd(111), Pd(100), and Pd(211) facets, finding higher energy barriers for the diffusion of dechlorinated carbon atoms (C*) on Pd(100) and Pd(211). Unable to escape, the accumulated C* on these facets might favor their poisoning by formation of PdC_x or coke. On the other hand, due to their multiple coordination options, some transition metals like Rh are prone to producing organometallic complexes. The chemisorption of reaction products and/or byproducts at the electro-deficient metal sites (which might be produced as in Scheme 1) may result in the production of organometallic complexes, covering the active metal centers [34].

6.2.2. Sintering of Active Centers

The sintering of the active centers has been commonly responsible of metallic catalyst deactivation in HDC studies [31,34,44,48,88,185–187]. The reduction temperature used during the catalysts' activation plays an important role in the dispersion of the metallic phase. As pointed out in Sections 3 and 4, temperatures of up to 400 °C are used for catalyst reduction and/or HDC reaction. The use of high reaction temperatures to enhance catalyst activity may lead to the mobility of the metallic particles to form larger aggregates, decreasing the available active surface [19,45,46]. Nevertheless, the resistance to sintering highly depends on the metal nature. In a recent study devoted to the HDC of DCM with carbon supported catalysts, Pd was found to be more prone to sintering, followed by Pt, whilst Rh showed the highest resistance to it [46]. Besides, the extent of metal sintering might also be related to the nature of the support, since the different interaction with HCl may promote metal particles' migration, resulting in metal sintering [35,188] or metal re-dispersion [168,189].

6.2.3. Formation of Carbonaceous Deposits

Another important deactivation agent is the formation of carbonaceous deposits or coke, many times including chlorine in their composition, blocking the porous structure of the catalysts and even poisoning the active phase [1,22,25,51,55,57,60,66,73,87,90,136,138,159,168,187,189–194]. The effect is usually observed thanks to a dramatic decrease in the surface area of the catalyst after the HDC (Table 3).

Table 3. Specific surface area of the catalysts before and after used in the HDC reactions.

CM	Catalyst	S_{BET} (m^2 g^{-1})		Ref.
		Before HDC	After HDC	
DCM	Rh/C	1110	1098	[1]
	Ru/C	1116	941	
TCM	Rh/C	1110	260	
	Ru/C	1116	404	
TTCM	Pt/Al_2O_3	95	62	[66]
	Pt/MgO	169	45	[70]
	Pd/Sibunit	335	185	[75]
	Pd/TiO_2	186	128	

Since coke may initiate via the decomposition and/or condensation of hydrocarbons on the catalytic surface [167], the extent of these deposits depends on different factors, such as the reaction temperature, the concentration of chloromethane used or the nature of the catalytic support. The HCl produced during the HDC may interact with inorganic supports like Al_2O_3, SiO_2, MgO or TiO_2, forming halides (Lewis acids), resulting in an increase in surface acidity [25,59,109,195]. Increasing the surface acidity and pore size of the catalyst favors the formation of these carbon deposits [74,81,167,168,183,190,196]. Organic supports like activated carbons, more resistant to HCl poisoning [28,172], do not suffer the increase in surface acidity observed in inorganic solids. The presence of organic or inorganic chlorinated species might even modify the electronic structure of the metal, producing new active centers [25]. As a result, oligomers, organometallic complexes or reaction reactants and products may be irreversibly adsorbed (quimisorbed) on the catalyst surface, favoring coupling reactions, and blocking the porous and active structure of the catalyst [25,34,36,43,159]. The favorable chemisorption of chloromethanes on the M^{n+} species has been observed not only experimentally, but through DFT molecular simulation calculations [31]. Nevertheless, the use of high concentrations of hydrogen has proven to minimize the deposition of chemisorbed species [197,198].

6.3. Regeneration of Catalysts

Although the deactivated catalysts might be regenerated, this strategy has been scarcely investigated in the literature, for which two different methods have been followed in HDC reactions: (i) in situ gas flow methods, and (ii) washing methods. The effects of the regeneration treatments depend on the catalyst employed and the main deactivation cause. The in-situ regeneration methods are technically simpler than the washing methods, and thus, have been more commonly explored, using H_2, O_2, air or inert gases like Ar [25,29,34,73,75,97,194]. O_2, air and Ar flows at different temperatures have been used to remove carbonaceous deposits or coke. Air flow at a temperature below 400 °C, was successfully used by González et al. [25] to regenerate some Pd/TiO_2 catalysts deactivated during the HDC of chloromethanes due to the formation of carbonaceous deposits. Liu et al. [29] also used an air flow (250 °C) to recover the Pd active centers deactivated by PdC_x. Furthermore, the same treatment was used by Martin-Martinez et al. [34] to remove the chlorinated organic compounds deposited on Rh and Ru catalysts (building organometallic complexes with those metals), blocking the catalysts' porous structure. Golubina et al. [75] studied the HDC of TTCM and were able to remove the carbonaceous deposits on their Pd/TiO_2 catalyst using an Ar flow treatment. On the other hand, H_2 flow has been found to be inappropriate for the removal of carbonaceous deposits [73], but should be useful for the removal of chlorine species [194]. Ordoñez et al. [194] tested H_2 and air flows to regenerate a Pd/Al_2O_3 catalyst deactivated during the HDC of tetrachloroethylene (TTCE) due to HCl poisoning and the formation of carbonaceous deposits, partially recovering the initial catalytic activity after both treatments. Among the washing methods, Ordoñez et al. [194] tried the washing of their deactivated catalysts using DCM, toluene, tetrahydrofurane or ammonia, but none of the treatments resulted effective. On the contrary, NaOH and ammonia have proven to be suitable for the removal of deposits deactivating Pd, Pd-Pt and Pd-Rh catalysts [154].

7. Summary and Outlook

Throughout this review, a global analysis of the HDC of chloromethanes has been presented, evidencing that HDC is a promising technology with potential industrial application in the removal of chloromethanes from industrial waste streams. For this issue, heterogeneous catalysts based on noble metals should preferably be used, owing to their excellent dechlorination and hydrogenation abilities. The method and conditions used for the synthesis of the catalysts affect the metal particles' size, their oxidation state, and their accessibility and distribution over the support. These properties, along with the structure, acidity and surface functional groups on the support, influence the catalytic activity. Modifying these properties and the operation conditions, the HDC may be pushed towards the complete removal of the chloromethanes and their selective transformation into hydrocarbons or

smaller chloromethanes. The reaction selectivity could be driven to obtain products of high industrial interest. Nevertheless, with a few exceptions, most catalysts suffer a serious deactivation during the HDC, mainly caused by poisoning, sintering of the active centers, and/or formation of deposits blocking the porous structure. Despite different treatments have proven their efficiency to regenerate the deactivated catalysts, especially some in situ gas flow methods using air, Ar or H_2, improving catalytic stability is imperative for the industrial application of this technology. Moreover, overcoming the problem of the presence of oxygen in exhaust gas streams is mandatory. Thus, in this final section, the future perspectives of this technology are explored, approaching the improvement of catalytic stability, the possible use of this technology for the upgrading of chloromethanes and a possible strategy for applying HDC in the presence of oxygen.

7.1. Improving Catalytic Stability

As has been illustrated, one of the main challenges for the potential industrial application of HDC of chloromethanes is to improve catalysts' stability. In this regard, we have learned that preparing catalysts containing M^0 particles, with a homogeneous size of around 2–3 nm and uniform distribution over a non-acidic organic support, might prevent catalysts' deactivation. Smaller particles and inorganic supports have less resistance to HCl poisoning [28,52,55,120,123,124,172]; M^{n+} species and larger particles are more prone to deactivation by oligomerization, coke, formation of metallic carbides or irreversible adsorption of the chloromethanes [29,31,34,35,37,48,85,127]; and the presence of acid centers in the support also favors the formation of coke [40,41,48,51,53,60,66,136–138]. Thus, in the near future it would be interesting to develop new methods for the synthesis of catalysts capable of controlling these parameters. Besides, it is important to understand the role of the different metal structures in which the active phase can be found, and the function that the exposed facets or created vacancies in the active centers may have in the catalysts deactivation. On the other hand, it seems important to operate using relatively smooth reaction temperatures to prevent metal sintering and high concentrations of hydrogen to minimize the deposition of chemisorbed species [19,35,45,46,166,188,197,198].

7.2. Upgrading of Chloromethanes

As we have discussed in the previous sections, the HDC process has proven to be a promising and powerful technology to transform the chloromethanes into non-chlorinated hydrocarbons, which are less hazardous and much more valuable industrial compounds.

7.2.1. Recycling of Chloromethanes into CH_4 Using HDC

Methane, as the main component of natural gas, is one of the most important fossil fuels. It may be used to produce syngas [199,200] or other important chemical components for industry, like methanol [201] and acetylene [202,203]. According to many experimental studies, methane is one of the main products obtained in the HDC of chloromethanes [29,39,46,47,49,50,74,86,93,204]. Selectivities of methane of around 90% and almost complete chloromethane conversions have been reported for the HDC of TTCM [74], TCM [1,31,33,50] and DCM [31,33], using temperatures ranging from 120 °C (HDC of TTCM with Pt/zeolite) [74] to 250 °C (HDC of DCM and TCM with Pt/C) [1,31,33]. Furthermore, the high selectivity to methane in the HDC of chloromethanes has also been verified in some DFT calculation studies [26,205]. Lang et al. [26] studied the mechanism of the HDC of TCM over Pd. They calculated the binding energies and the activation energy barriers of TCM and all the reaction intermediates, finding that methane was the more favorable product obtained, independently of the crystalline structure of Pd.

7.2.2. An Alternative Route for the Production of Olefins from Waste Gas Streams

In modern chemical industries, light olefins, especially ethylene and propylene, are used as important chemical building blocks, with a growing market demand. Frequently, light olefins are produced by the steam cracking of naphtha in petrochemical industry. In recent years, however,

with the decrease in petroleum sources, the development of new production routes for olefins, using alternative raw materials, is being highly demanded. Some emerging routes such as methanol to olefins (MTO) [206,207] have drawn increasing attention. However, methanol is mainly produced by the reforming of steam methane to syngas, usually a high energy cost process [208].

In recent years, the use of chloromethanes for the production of olefins has become an attractive alternative route. MCM has been widely employed as an intermediate in a two-step method to produce olefins from methane (Scheme 4) [209–230], usually employing zeolytic catalysts with chabazite-type structure (silicoaluminophosphates (SAPO) [209–221] and zeolite socony mobils (ZSM) [220–230]).

$$CH_4 + HCl + \frac{1}{2}O_2 \rightarrow CH_3Cl + H_2O \quad \text{(Step 1)}$$

$$CH_3Cl \rightarrow \frac{1}{n}C_nH_{2n(n=2-4)} + HCl \quad \text{(Step 2)}$$

Scheme 4. Two-step method to transform methane into light olefins [231].

Nevertheless, during the process, the generation of byproducts such as DCM and TCM is inevitable. Hence, exploring the transformation of these byproducts (DCM and TCM) into light olefins seems necessary to enhance the global efficiency of this process.

Transforming DCM into Olefins:

DCM is one of the main byproducts obtained in the methane transformation into light olefins [20]. Saadun et al. [45] explored the conversion of DCM into MCM, which could further continue to produce olefins (Figure 6), employing Ir-based catalysts. They suggested that the catalysts could exhibit an unparalleled selectivity to MCM (around 95%) with a significant stability. However, the conversion of DCM was low (ca. 25%).

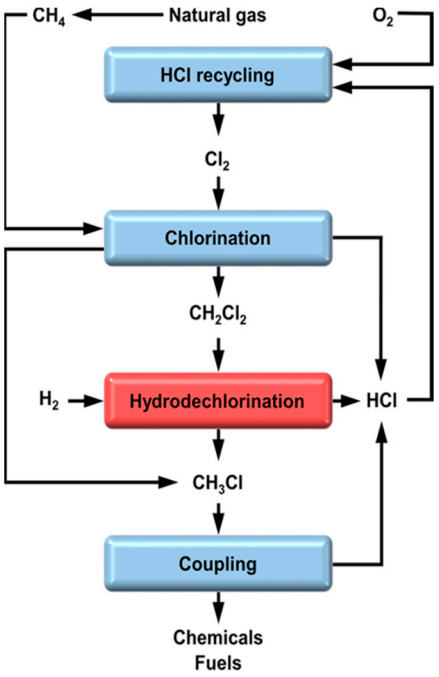

Figure 6. Simplified process flow diagram of valorization of methane using MCM and DCM as intermediates. Reprinted with permission from ref. [45].

Moreover, Gómez-Sainero et al. [33], formulated a new attractive idea to transform DCM into olefins in a single step, employing the HDC reaction. They first accomplished a DFT calculation study,

to anticipate the catalytic performance of Pd, Pt, Ru and Rh in the HDC of DCM. Their study included the estimation of barrier energies for the adsorption, reaction and desorption of reactants (DCM and H_2) and products, in order to determine possible intermediates and products that would be obtained during the HDC of DCM over metallic catalysts represented as octahedral clusters with zero charge. The production of the main products (CH_4, C_2H_4 and C_2H_6) was exothermic. All the four clusters were able to dechlorinate a single DCM molecule and obtain a stable $^{\bullet\bullet}CH_2$ radical, not suffering any remarkable geometrical deformation. Nevertheless, when expanded the system to 2 DCM and 3 H_2 molecules, only the Pd_6 and Rh_6 clusters allowed the obtaining of stable radical intermediates. A better performance should be expected with the Rh_6 cluster, since it showed higher stabilization energies than Pd_6 for the adsorption of the intermediates on the cluster. However, the lowest desorption energies for ethane and ethylene were obtained with Pd_6, identifying this metal as the most favorable to produce the desired C2 products. The theoretical description of the reaction mechanism over Pd_6 clusters (Figure 7) showed a preferred selectivity in the order $CH_4 > C_2H_6 > C_2H_4$, according to their thermodynamic stability. Based on these results, they performed an experimental HDC study, which agreed with the computational results. Pd catalyst showed the best performance to obtain C2 products by HDC of chloromethanes, with yields of ca. 80% at 400 °C in the HDC of TCM, against 44%, 36% and 4% obtained with Rh, Ru and Pt, respectively. This remarkable ability of Pd to produce C1+ hydrocarbons has been observed in several experimental HDC studies [28,32,33,37,39,48–50,52,69,75,76,87,93,232,233].

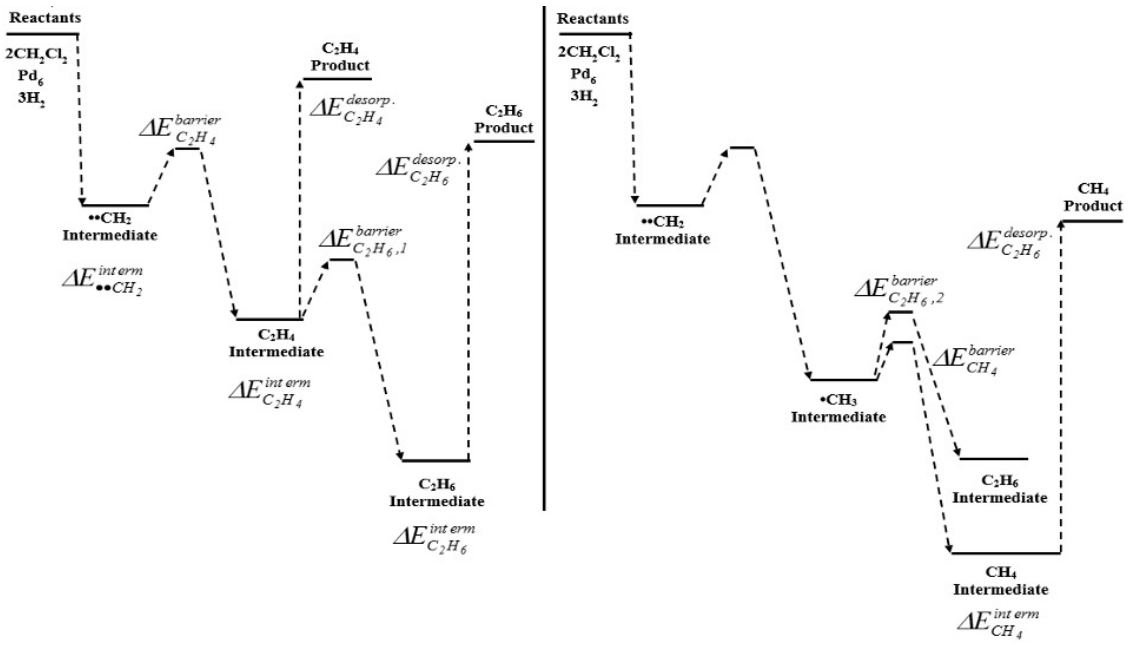

Figure 7. Scheme of reaction mechanism for the HDC of DCM obtained by quantum-chemical calculations for Pd. Reprinted with permission from ref. [33].

Fernandez-Ruiz et al. [32] investigated the performance of Pd catalysts supported on different zeolytic materials in the HDC of DCM. According to their analysis, zeolites with lower surface acidity promoted the distribution of Pd into bigger particles, favoring the selectivity to olefins. Besides, in order to increase the selectivity to these unsaturated hydrocarbons, the authors decreased the concentration of H_2 (molar ratios H_2/DCM from 100 to 10 were tested), and increased the reaction temperature (the range 75–300 °C was tested), obtaining ca. 40% olefins, mainly C_2H_4 and C_3H_6, with the lowest H_2/DCM molar ratio at 300 °C. Therefore, the near future studies should focus on the development of non-acidic catalysts with small and well-dispersed Pd particles, to facilitate the production of light olefins, assuring high DCM conversions.

Transforming TCM into Olefins:

Using DFT calculations, Xu et al. [26] determined that, in the HDC of TCM over Pd(111), Pd(100) and Pd(211) facets, TCM might fully dechlorinate, and methane should be the main reaction product obtained (Figure 8). They claimed that the intermediates involved in the production of other hydrocarbons might hardly be hydrogenated due to their higher activation energy barriers (Figure 8), and did not consider the formation of C1+ products. However, if the hydrogenation extent could be controlled using suitable operating condition, C1+ dechlorinated products like C_2H_4 and C_2H_6 might be obtained [32,33,48].

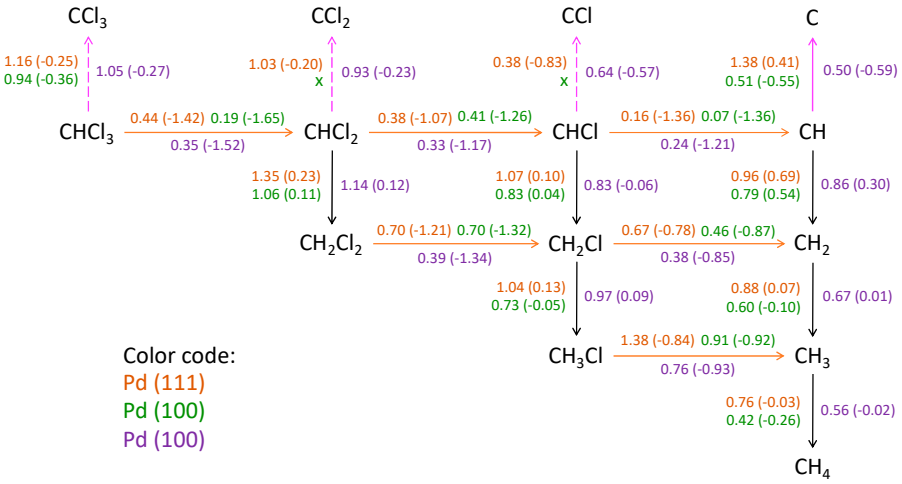

Figure 8. Activation energy barriers (in eV, outside the parentheses) and reaction energies (in eV, inside the parentheses) of surface elementary reaction steps. Orange arrows: dechlorination; black arrows: hydrogenation; pink arrows: dehydrogenation. Dashed arrows: dehydrogenation steps energetically unfavorable. "X": it was unable to determine any feasible reaction path. Reprinted with permission from ref. [26].

As observed for DCM, the production of olefins through the HDC of TCM is thermodynamically more favorable at relatively higher temperatures [33] and low H_2/chloromethane ratios [32], using Pd catalysts [33] and non-acidic supports [32]. Besides, the presence of some surface functional groups has been identified to contribute to the selectivity of the process. Larger amounts of surface oxygenated groups, in the support, viz. carbonyl and quinone, have been identified as promoters of the adsorption of reactants and intermediates in the catalyst, resulting in the complete hydrogenation of the intermediates [48]. In a recent study, five Pd catalysts supported in different activated carbons were evaluated, finding that supports with low concentrations of these surface oxygenated groups led to high selectivities to olefins, ca. 65% (300 °C, H_2/TCM 50). On the contrary, carbons with larger amounts of oxygenated groups contributed to the formation of saturated hydrocarbons. They correlated the presence of the aforementioned oxygenated surface groups with the higher proportion of electro-deficient Pd (Pd^{n+}) species in the catalyst, also identifying this Pd^{n+} as a promoter of catalyst deactivation, due to the chemisorption of chlorides on this specie, poisoning the active sites [48]. A similar result was obtained by Martin-Martinez et al. [34]. They regenerated some Rh and Ru catalysts that were highly deactivated after the HDC of TCM. After a regeneration treatment with air at 250 °C, both catalysts recovered their initial activity, showing higher selectivities to olefins and lower selectivities to paraffins. By comparing the distribution of the oxygenated species on the fresh and regenerated catalysts, higher contents of C-O groups (epoxy and hydroxyl groups) and lower contents of C=O groups (carbonyl, carboxyl and carboxylate groups) were found in the regenerated catalysts. All these results suggest that the presence of C=O groups might favor the hydrogenation of olefins to saturated hydrocarbons, while C-O groups have lower hydrogenation ability.

In conclusion, Pd catalysts may be valuable for the upgrading of TCM and DCM into light olefins by HDC. The active phase should consist of small and well-dispersed metal particles. The catalytic support should not be acidic and should contain low concentrations of C=O groups to prevent the formation of paraffins from olefins. Furthermore, a low concentration of oxygenated species might also minimize the interactions with metal particles and reduce the formation of electro-deficient species, which have also proven to promote the catalyst deactivation and disfavor the formation of olefins. In addition, an appropriate increase in reaction temperature and decrease in H_2/chloromethane ratio helps the formation of olefins.

7.3. Application of Gas-Phase HDC in Industry

Attached to the chlorinated pollutants, real gaseous industrial waste streams may contain high concentrations of oxygen (up to 21% due to air atmosphere). Thus, it does not seem possible to carry on a treatment where important concentrations of H_2 and temperature are needed. Elola et al. [234] addressed this challenge, proposing a two step process (Figure 9). First, the adsorption of the chlorinated waste in a porous solid. Then, the regeneration of the adsorbent using a H_2 flow. They tested several adsorbents (zeolites, activated carbons, graphite and clays), loaded with 0.5 wt.% Pd. With the Pd-zeolite-KL, by this two-step methodology, the authors obtained almost complete conversion of trichloroethylene (92%), and almost total selectivity to ethane.

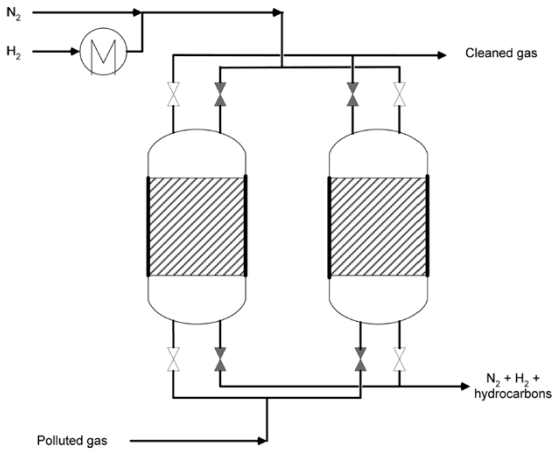

Figure 9. Scheme of adsorption/hydrodechlorination apparatus proposed by Elola et al. [234]: a first step of nitrogen flow in order to remove the oxygen, and a second step of hydrogen to hydrogenate the adsorbed chlorinated compounds. Reprinted with permission from ref. [234].

Author Contributions: Conceptualization, M.M.-M. and L.M.G.-S.; methodology, S.L., J.A.O., D.R.-F. and M.M.-M.; writing—original draft preparation, S.L. and J.A.O.; writing—review and editing, M.M.-M., J.J.R. and L.M.G.-S.; supervision, M.M.-M., J.J.R. and L.M.G.-S. All authors have read and agreed to the published version of the manuscript.

Funding: The authors gratefully acknowledge financial support through research projects SI1/PJI/2019-00487 (Comunidad de Madrid/UAM) and CTM2017-85498-R (FEDER/Ministerio de Ciencia, Innovación y Universidades-Agencia Estatal de Investigación). M. Martín Martínez acknowledges a postdoctoral grant, 2017-T2/AMB-5668, from the Comunidad de Madrid "Atracción de talento investigador" programme. S. Liu acknowledges MINECO for his research grant PRE2018-084424.

Conflicts of Interest: The authors declare no conflict of interest.

Appendix A

Table A1. Influence of operating conditions in the HDC of chloromethanes (CM). How to read this table: The first line for example, shows that the increasing of the reaction temperature from 150 to 250 °C, leads to an increase in conversion (from 20 to 95%), an increase in selectivity to CH_4+C2+C3+C4 (from 83 to 98%) and a decrease in selectivity to MCM (from 17 to 2%).

Catalyst	CM	Operation Conditions				Highest Conversion (%)	Highest Selectivity (%)						Ref.
		T (°C)	P (bar)	τ (*) (kg·h·mol^{-1})	H_2/CM (**)		CH_4	C2	C3	C4	MCM	DCM	TCM	
Influence of Reaction Temperature														
Pd-Pt(1:1.8)/AC	DCM	150→250	1	0.6	100	ca. 20→95		ca. 83→98			ca. 17→2	-	-	[37]
Pd-Pt(4:1)/AC	DCM	150→200	1	0.6	100	ca. 20→53	83.2→ 86.7	2.4→5	-	-	14.4→8.4	-	-	[85]
Pd-Pt(1:1)/AC	DCM	150→200	1	0.6	100	ca. 18→56	88.2→ 92.2	0→0.6	-	-	11.8→7.2	-	-	[85]
Pd-Pt(1:3)/AC	DCM	150→200	1	0.6	100	ca. 12→50	85.8→ 90.2	-	-	-	14.2→9.8	-	-	[85]
Pd(1wt.%)/AC	DCM	150→200	1	0.6	100	ca. 13→45	80.7→ 80.2	1.6→8	-	-	17.7→11.9	-	-	[85]
Pt(1wt.%)/AC	DCM	150→200	1	0.6	100	ca. 9→38	79.2→ 83.2	-	-	-	20.8→16.8	-	-	[85]
Pd(1wt.%)/AC	MCM	175→250	1	1.73	100	ca. 13→35				n/a				[1]
Pd(1wt.%)/AC	DCM	175→250	1	1.73	100	ca. 45→95	ca. 78→ 68	ca. 6→22	ca. 0→2	-	ca. 16→8	-	-	[1]
Pd(1wt.%)/AC	TCM	175→250	1	1.73	100	100	ca. 41	ca. 36	ca. 14	ca. 5	ca. 1	ca. 3	-	[1]
Pt(1wt.%)/AC	MCM	175→250	1	1.73	100	ca. 5→13				n/a				[1]
Pt(1wt.%)/AC	DCM	175→250	1	1.73	100	ca. 35→87	ca. 80→87	-	-	-	ca. 20→13	-	-	[1]
Pt(1wt.%)/AC	TCM	175→250	1	1.73	100	100	ca. 82→92	-	-	-	ca. 2→1	ca. 16→7	-	[1]
Rh(1wt.%)/AC	MCM	175→250	1	1.73	100	ca. 4→21				n/a				[1]
Rh(1wt.%)/AC	DCM	175→250	1	1.73	100	ca. 38→100	ca. 76→66	ca. 10→20	ca. 2→7	-	ca. 12→7	-	-	[1]
Rh(1wt.%)/AC	TCM	175→250	1	1.73	100	100	ca. 25→50	ca. 15→18	ca. 15→12	ca. 0→ 1	ca. 10→15	ca. 35→4	-	[1]
Ru(1wt.%)/AC	MCM	175→250	1	1.73	100	ca. 1→7				n/a				[1]
Ru(1wt.%)/AC	DCM	175→250	1	1.73	100	ca. 21→87	ca. 80→56	ca. 8→17	ca. 5→14	-	ca. 7→13	-	-	[1]
Ru(1wt.%)/AC	TCM	175→250	1	1.73	100	ca. 80→100	ca. 8→25	ca. 1→12	ca. 10→24	ca. 0	ca. 1→10	ca. 80→29	-	[1]
Pt(0.5wt.%)/WZ	DCM	150→250	1	0.8	100	ca. 8→80	ca. 63→61	ca. 0→11	ca. 0→5	ca. 18→1	ca. 19→22	-	-	[42]
Pt-Pd(1:1)/WZ	DCM	150→250	1	0.8	100	ca. 30→98	ca. 65→66	ca. 0→10	ca. 0→4	ca. 0→2	ca. 35→18	-	-	[42]
Pd(0.5wt.%)/WZ	DCM	150→250	1	0.8	100	ca. 30→90	ca. 55→62	ca. 0→10	ca. 0→5	ca. 3→1	ca. 42→22	-	-	[42]
Pt(0.5wt.%)/SZ	DCM	150→250	1	0.8	100	ca. 5→90	ca. 66→67	ca. 0→8	ca. 0→3	ca. 12→1	ca. 22→21	-	-	[42]
Pt-Pd(1:1)/SZ	DCM	150→250	1	0.8	100	ca. 10→80	ca. 68→88	ca. 0→1	ca. 0	ca. 5→0	ca. 27→12	-	-	[42]
Pd(0.5wt.%)/SZ	DCM	150→250	1	0.8	100	ca. 8→82	ca. 65→80	ca. 0→8	ca. 0→2	ca. 12→0	ca. 23→10	-	-	[42]
Pd(3wt.%)/HY	TTCM	120→400	1	10 mg *	40 ** cm^3H_2/min	16.3→91.9	9.7→23.8	61→50.6	23.4→22.1	1.3→1.5	-	1.0→0.2	0.3→0.1	[69]
Pd(3wt.%)/HZSM-5	TTCM	120→400	1	10 mg *	40 ** cm^3H_2/min	32.2→35.6	2.0→8.1	93→64.3	23.4→22.1	2.3→22	-	0→0.3	0.2→2.3	[69]
Pt(3wt.%)/HY	TTCM	120→400	1	10 mg *	40 ** cm^3H_2/min	76.1→58.9	22.4→67.6	48.7→28.8	0.9→1.3	0	-	1.8→0.4	25.6→1.7	[69]
Pt(3wt.%)/HZSM-5	TTCM	120→400	1	10 mg *	40 ** cm^3H_2/min	37.6→70.3	57.8→93.9	3.1→1.9	1.6→0.8	0→1.7	-	0→0.6	37.6→0.7	[69]
Pt(1wt.%)/AC	DCM	150→250	1	0.8	100	ca. 25→60	ca. 74→85	-	-	-	-	-	-	[35]
Pt(1wt.%)/AC	TCM	125→200	1	0.8	100	67→ 100	88.1→93.8	-	-	-	4.2→3.1	7.7→3.1	-	[35]
Pd(1wt.%)/AC	MCM	150→250	1	0.6	100	ca. 8→25				n/a				[28]
Pd(1wt.%)/AC	DCM	150→250	1	0.6	100	ca. 10→85	79.9→64.5	3.1→26.6	0→1.6	-	17→7.3	-	-	[28]
Pd(1wt.%)/AC	TCM	125→175	1	0.6	100	ca. 99→100	52.7→41.4	28.3→37.4	8.9→12.9	3→4.7	2.4→1.1	4.7→2.5	-	[28]
Pd(0.5wt.%)/SiO_2	TCM	100→225	1	0.1 g *	9.5	ca. 2→98	ca. 75→40	ca. 18→40	ca. 5→13	ca. 2→7	-	-	-	[87]
Pt(0.5wt.%)/AC	TCM	140→240	1	8 mg *	8 ***	34→93	47→68	-	-	-	-	53→32	-	[50]
Pt(1wt.%)/η-Al_2O_3	TCM	140→240	1	8 mg *	8 ***	27→89	70→77	-	-	-	-	30→23	-	[50]

Table A1. *Cont.*

Catalyst	CM	Operation Conditions				Highest Conversion (%)	Highest Selectivity (%)						Ref.
		T (°C)	P (bar)	τ (*) (kg·h·mol^{-1})	H_2/CM (**)		CH_4	C2	C3	C4	MCM	DCM	TCM	
Pt(0.4wt.%)/Vycor	TCM	240→260	1	8 mg *	8 ***	38→52	74→83	-	-	-	-	26→17	-	[50]
Pt(1wt.%)/AlF_3	TCM	180→260	1	8 mg *	8 ***	4→78	55→84	-	-	-	-	45→16	-	[50]
Pd(0.5wt.%)/AC	TCM	140→180	1	2 g *	7.35 ***	9→94	58→88	-	-	-	-	42→12	-	[50]
Pt-Pd(1:1)/SZ	DCM	150→250	1	0.8	100	ca. 10→81	ca. 70→85	ca. 0→1	0	ca. 5→0	ca. 25→14	-	-	[21]
Pt-Pd(3:1)/SZ	DCM	150→250	1	0.8	100	ca. 8→58	ca. 62→70	ca. 1→3	ca. 0→6	ca. 7→1	ca. 30→20	-	-	[21]
Pt-Pd(1:3)/SZ	DCM	150→250	1	0.8	100	ca. 8→85	ca. 69→87	ca. 1→2	0→1	ca. 1→0	ca. 29→10	-	-	[21]
Pt-Pd(1:3)/SZ	TCM	150→250	1	0.8	100	ca. 70→98	ca. 82→75	ca. 10→16	ca. 3→6	ca. 0→2	ca. 0	ca. 5→1	-	[21]
Pt/C	DCM	200→400	1	0.8	10	ca. 15→88	ca. 86→95	ca. 0	ca. 0	ca. 0	ca. 14→5	-	-	[33]
Pt/C	TCM	200→400	1	0.8	10	ca. 96→100	ca. 96→98	ca. 0→2	ca. 0	ca. 0	ca. 0	ca. 4→0	-	[33]
Ru/C	DCM	150→400	1	0.8	10	ca. 16→100	ca. 80→64	ca. 10→28	ca. 5→4	ca. 0	ca. 5→4	-	-	[33]
Ru/C	TCM	150→400	1	0.8	10	ca. 19→95	ca. 19→45	ca. 15→35	ca. 0	ca. 19→0	ca. 2→5	ca. 45→15	-	[33]
Pd/C	DCM	150→400	1	0.8	10	ca. 22→95	ca. 85→54	ca. 5→44	ca. 0	ca. 0	ca. 10→2	-	-	[33]
Pd/C	TCM	150→400	1	0.8	10	ca. 90→100	ca. 52→20	ca. 32→75	ca. 10→1	ca. 0	ca. 1→4	ca. 5→0	-	[33]
Rh/C	DCM	150→400	1	0.8	10	ca. 25→100	ca. 82→67	ca. 8→27	ca. 2→6	ca. 0	ca. 8→0	-	-	[33]
Rh/C	TCM	150→400	1	0.8	10	ca. 55→93	ca. 45→42	ca. 16→42	ca. 16→2	ca. 0→1	ca. 8→1	ca. 15→12	-	[33]
Pt(25wt.%)/CNT	TTCM	70→90	1	0.018 g *	7	39→95	19.5→22	1.4→0.4	0.2→0	-	ca. 0.4→0	-	76.5→77	[138]
Pd(2wt.%)/MgO	TTCM	120→250	1	0.2 g *	10	0→10				n/a				[142]
Pd(0.6wt.%)/Al_2O_3	DCM	100→400	1	0.005 * g min mL^{-1}	10	ca. 10→99				n/a				[30]
Ni (0.6 wt.%)/Al_2O_3	DCM	100→400	1	0.005 * g min mL^{-1}	10	ca. 9→99				n/a				[30]
Influence of Pressure														
Ni-Mo/γ-Al_2O_3	DCM	350	20→100	1 g *	3.26 ***	ca. 65→100				n/a				[40]
Pt(0.5 wt.%)/γ-Al_2O_3	TTCM	130	1→9	4500 L/kg·h *	11	99.3→99.9	32.4→18.4	-	-	-	-	0.08→0.6	65.2→79.3	[56]
Influence of Space Time														
Pd(1wt.%)/AC	MCM	250	1	0.04→1.73	100	ca. 5→35	-	-	-	-	-	-	-	[1]
Pd(1wt.%)/AC	DCM	250	1	0.04→1.73	100	ca. 20→95	ca. 65→68	ca. 30→22	ca. 2→1	-	ca. 3→9	-	-	[1]
Pd(1wt.%)/AC	TCM	250	1	0.04→1.73	100	ca. 99→100	ca. 25→20	ca. 48→50	ca. 18→19	ca. 6→8	ca. 0	ca. 3	-	[1]
Pt(1wt.%)/AC	MCM	250	1	0.04→1.73	100	ca. 4→13				n/a				[1]
Pt(1wt.%)/AC	DCM	250	1	0.04→1.73	100	ca. 5→85	ca. 90→89	-	-	-	ca. 10→11	-	-	[1]
Pt(1wt.%)/AC	TCM	250	1	0.04→1.73	100	ca. 40→100	ca. 92→91	-	-	-	ca. 1.5	ca. 6.5→7.5	-	[1]
Rh(1wt.%)/AC	MCM	250	1	0.04→1.73	100	ca. 4→23				n/a				[1]
Rh(1wt.%)/AC	DCM	250	1	0.04→1.73	100	ca. 20→100	ca. 66→65	ca. 22→23	ca. 6	-	ca. 6	-	-	[1]
Rh(1wt.%)/AC	TCM	250	1	0.04→1.73	100	ca. 18→100	ca. 15→50	ca. 12→18	ca. 8→12	ca. 3→0	ca. 0→15	ca. 62→5	-	[1]
Ru(1wt.%)/AC	MCM	250	1	0.04→1.73	100	ca. 2→7				n/a				[1]
Ru(1wt.%)/AC	DCM	250	1	0.04→1.73	100	ca. 8→85	ca. 50→51	ca. 25→26	ca. 15→10	-	ca. 10→13	-	-	[1]
Ru(1wt.%)/AC	TCM	250	1	0.04→1.73	100	ca. 10→100	ca. 0→28	ca. 0→15	ca. 0→15	ca. 0	ca. 0→12	ca. 100→30	-	[1]
Pd(1wt.%)/AC	MCM	250	1	0.08→1.73	100	ca. 5→34				n/a				[28]
Pd(1wt.%)/AC	DCM	250	1	0.08→1.73	100	ca. 28→95	62.7→67.9	27.9→23.9	2.2→1.4	-	7.2→6.8	-	-	[28]
Pd(1wt.%)/AC	TCM	175	1	0.08→1.73	100	ca. 68→100	32.7→42.7	38.2→34.5	27.1→13.3	7.5→5.3	1.5→1.2	3.0	-	[28]
Pd(0.5wt.%)/AC	DCM	250	1	1→6.6	400	ca. 60→92	ca. 85→80	ca. 2→5	-	-	ca. 13→15	-	-	[39]

Table A1. *Cont.*

Catalyst	CM	Operation Conditions				Highest Conversion (%)	Highest Selectivity (%)						Ref.
		T (°C)	P (bar)	τ (*) (kg·h·mol^{-1})	H_2/CM (**)		CH_4	C2	C3	C4	MCM	DCM	TCM	
Pd-Pt(1:1.8)/AC	DCM	250	1	0.08→2.5	50	40→100		ca. 40→99			-	-	-	[37]
Pt(1wt.%)/AC	DCM	250	1	0.08→1.73	100	ca. 35→70	ca. 86→84	-	-	-	-	-	-	[35]
Pd(0.5wt.%)/Al_2O_3	DCM	300	1	0.4→1.8	10	ca. 10→28				n/a				[19]
Influence of H_2/CM Molar Ratio														
Pd-Pt(1:1.8)/AC	DCM	250	1	0.6	25→200	ca. 90→98		ca. 99→95			ca. 1→5	-	-	[37]
Pd(0.5wt.%)/AC	DCM	250	1	3.5	50→400	ca. 65→80				n/a				[39]
Pd(0.5wt.%)/Al_2O_3-c	DCM	200	1	0.005 * g min mL^{-1}	3→10	ca. 50→60				n/a				[30]
Pd(0.5wt.%)/Al_2O_3	DCM	200	1	0.005 * g min mL^{-1}	3→10	ca. 40→60				n/a				[30]
Ni(0.5wt.%)/Al_2O_3	DCM	200	1	0.005 * g min mL^{-1}	3→10	ca. 28→32				n/a				[30]
Pd(0.6wt.%)/Al_2O_3	DCM	200	1	0.005 * g min mL^{-1}	3→10	ca. 22→32				n/a				[30]
Ni(0.6wt.%)/Al_2O_3	DCM	200	1	0.005 * g min mL^{-1}	3→10	ca. 28→32				n/a				[30]
Al_2O_3	DCM	200	1	0.005 * g min mL^{-1}	3→10	ca. 18→32				n/a				[30]
Pt(1.5wt.%)/Al_2O_3	TTCM	90	1	0.26 s *	6.7→13.4	ca. 9→11	ca. 5→8			ca. 55→2			ca. 40→90	[55]
Pt(1.5wt.%)/Al_2O_3	TTCM	90	1	0.26 s *	21.7→4.8	ca. 96→46	ca. 28→22			ca. 0			ca. 72→78	[55]
Pt(0.5 wt.%)/γ-Al_2O_3	TTCM	130	6	4500 L/kg·h *	9→15	100	28.4→24.3	-	-	-	-	0.75→0.72	68.6→73.5	[56]

n/a no data available; ca. approximate data read from figures; * space time in [kg h mol^{-1}]; space velocity in [g min mL^{-1}] or [L kg^{-1} h^{-1}]; mass of catalysts in [g]; contact time in [s]; ** molar ratio H_2/CM adimensional; H_2 flow in [cm^3 min^{-1}] in the liquid-phase HDC; *** data calculated from reactants flows given in the cited references.

References

1. Martin-Martinez, M.; Gómez-Sainero, L.; Alvarez-Montero, M.; Bedia, J.; Rodriguez, J. Comparison of different precious metals in activated carbon-supported catalysts for the gas-phase hydrodechlorination of chloromethanes. *Appl. Catal. B Environ.* **2013**, *132–133*, 256–265. [CrossRef]
2. Huang, B.; Lei, C.; Wei, C.; Zeng, G. Chlorinated volatile organic compounds (Cl-VOCs) in environment—Sources, potential human health impacts, and current remediation technologies. *Environ. Int.* **2014**, *71*, 118–138. [CrossRef] [PubMed]
3. Schlosser, P.M.; Bale, A.S.; Gibbons, C.F.; Wilkins, A.; Cooper, G.S. Human Health Effects of Dichloromethane: Key Findings and Scientific Issues. *Environ. Health Perspect.* **2015**, *123*, 114–119. [CrossRef] [PubMed]
4. Tolman, K.G.; Dalpiaz, A.S. Occupational and Environmental Hepatotoxicity. In *Drug-Induced Liver Disease*, 3rd ed.; Elsevier: Amsterdam, The Netherlands, 2013; Chapter 36; pp. 659–675.
5. Derwent, R.G.; Hester, R.E.; Harrison, R.M. Sources, distributions, and fates of VOCs in the atmosphere. In *Issues in Environmental Science and Technology*; Royal Society of Chemistry (RSC): Cambridge, UK, 2007; pp. 1–16.
6. The Montreal Protocol on Substances that Deplete the Ozone Layer. Article 2C: Carbon Tetrachlroride. Available online: https://ozone.unep.org/treaties/montreal-protocol/articles/article-2d-carbon-tetrachloride?q=es/treaties/montreal-protocol/articles/articulo-2d-tetracloruro-de-carbono (accessed on 25 April 2020).
7. Department of the Environment, Water, Heritage and the Arts. Universal Ratification of the Montreal Protocol. 2009. Available online: https://www.environment.gov.au/protection/ozone/publications/universal-ratification-montreal-protocol (accessed on 10 December 2020).
8. Regulation (EC) No 166/2006 of the European Parliament and of the Council of 18 January 2006. Available online: https://eur-lex.europa.eu/legal-content/HR/TXT/?uri=CELEX:32006R0166 (accessed on 5 September 2020).
9. CFR Part 63. National Air Emission Standards for Hazardous Air Pollutants: Halogenated Solvent Cleaning; Final Rule of the Environmental Protection Agency of 3 May 2007. 2007. Available online: https://www.epa.gov/stationary-sources-air-pollution/halogenated-solvent-cleaning-national-emission-standards-hazardou-0#rule-summary (accessed on 5 September 2020).
10. Yuan, G.; Keane, M.A. Liquid phase catalytic hydrodechlorination of chlorophenols at 273 K. *Catal. Commun.* **2003**, *4*, 195–201. [CrossRef]
11. Taylor, P.H.; Dellinger, B. Thermal degradation characteristics of chloromethane mixtures. *Environ. Sci. Technol.* **1988**, *22*, 438–447. [CrossRef]
12. Kovalchuk, V.I.; D'Itri, J.L. Catalytic chemistry of chloro- and chlorofluorocarbon dehalogenation: From macroscopic observations to molecular level understanding. *Appl. Catal. A Gen.* **2004**, *271*, 13–25. [CrossRef]
13. Hannus, I.; Halász, J. Hydrodechlorination over Zeolite Supported Catalysts—Clarification of Reaction Mechanism. *J. Jpn. Pet. Inst.* **2006**, *49*, 105–113. [CrossRef]
14. Rhodes, C.J. Zeolite Mediated Reactions: Mechanistic Aspects and Environmental Applications. *Prog. React. Kinet. Mech.* **2008**, *33*, 1–79. [CrossRef]
15. Dai, C.; Zhou, Y.; Peng, H.; Huang, S.; Qin, P.; Zhang, J.; Yang, Y.; Luo, L.; Zhang, X. Current progress in remediation of chlorinated volatile organic compounds: A review. *J. Ind. Eng. Chem.* **2018**, *62*, 106–119. [CrossRef]
16. Hu, M.; Liu, Y.; Yao, Z.; Ma, L.; Wang, X. Catalytic reduction for water treatment. *Front. Environ. Sci. Eng.* **2017**, *12*. [CrossRef]
17. Won, Y.S. Thermal stability and reaction mechanism of chloromethanes in excess hydrogen atmosphere. *J. Ind. Eng. Chem.* **2007**, *13*, 400–405.
18. Wu, Y.-P.; Won, Y.-S. Pyrolysis of chloromethanes. *Combust. Flame* **2000**, *122*, 312–326. [CrossRef]
19. López, E. Kinetic study of the gas-phase hydrogenation of aromatic and aliphatic organochlorinated compounds using a Pd/Al2O3 catalyst. *J. Hazard. Mater.* **2003**, *97*, 281–294. [CrossRef]
20. Kartashov, L.M.; Rozanov, V.N.; Treger, Y.A.; Flid, M.R.; Kalyuzhnaya, T.L.; Tkach, D.V. Processing the wastes from the production of methyl chloride in the synthesis of olefins from natural gas. *Catal. Ind.* **2010**, *2*, 230–238. [CrossRef]

21. Bedia, J.; Arevalo-Bastante, A.; Grau, J.; Dosso, L.; Rodriguez, J.; Mayoral, A.; Diaz, I.; Gómez-Sainero, L. Effect of the Pt–Pd molar ratio in bimetallic catalysts supported on sulfated zirconia on the gas-phase hydrodechlorination of chloromethanes. *J. Catal.* **2017**, *352*, 562–571. [CrossRef]
22. Rhodes, W.D.; Kovalchuk, V.I.; McDonald, M.A. Reaction pathways of halocarbon catalytic oligomerization. *Catal. Commun.* **2012**, *18*, 98–101. [CrossRef]
23. Arevalo-Bastante, A.; Álvarez-Montero, M.A.; Bedia, J.; Gómez-Sainero, L.; Rodríguez, J.J. Gas-phase hydrodechlorination of mixtures of chloromethanes with activated carbon-supported platinum catalysts. *Appl. Catal. B Environ.* **2015**, *179*, 551–557. [CrossRef]
24. Sánchez, C.A.G.; Patiño, C.O.M.; De Correa, C.M. Catalytic hydrodechlorination of dichloromethane in the presence of traces of chloroform and tetrachloroethylene. *Catal. Today* **2008**, *133*, 520–525. [CrossRef]
25. González, C.A.; Bartoszek, M.; Martin, A.; De Correa, C.M. Hydrodechlorination of Light Organochlorinated Compounds and Their Mixtures over Pd/TiO2-Washcoated Minimonoliths. *Ind. Eng. Chem. Res.* **2009**, *48*, 2826–2835. [CrossRef]
26. Xu, L.; Bhandari, S.; Chen, J.; Glasgow, J.; Mavrikakis, M. Chloroform Hydrodechlorination on Palladium Surfaces: A Comparative DFT Study on Pd(111), Pd(100), and Pd(211). *Top. Catal.* **2020**, *63*, 762–776. [CrossRef]
27. Ordóñez, S.; Sastre, H.; Díez, F.V. Hydrodechlorination of aliphatic organochlorinated compounds over commercial hydrogenation catalysts. *Appl. Catal. B Environ.* **2000**, *25*, 49–58. [CrossRef]
28. Álvarez-Montero, M.; Gómez-Sainero, L.; Martín-Martínez, M.; Heras, F.; Rodriguez, J. Hydrodechlorination of chloromethanes with Pd on activated carbon catalysts for the treatment of residual gas streams. *Appl. Catal. B Environ.* **2010**, *96*, 148–156. [CrossRef]
29. Liu, S.; Martin-Martinez, M.; Álvarez-Montero, M.A.; Arevalo-Bastante, A.; Rodríguez, J.J.; Gómez-Sainero, L. Recycling of Gas Phase Residual Dichloromethane by Hydrodechlorination: Regeneration of Deactivated Pd/C Catalysts. *Catalysts* **2019**, *9*, 733. [CrossRef]
30. Zuluaga, B.H.A.; González, C.A.; Barrio, I.; Montes, M.; De Correa, C.M. Screening of Pd and Ni supported on sol–gel derived oxides for dichloromethane hydrodechlorination. *J. Mol. Catal. A Chem.* **2004**, *222*, 189–198. [CrossRef]
31. Martin-Martinez, M.; Álvarez-Montero, A.; Gómez-Sainero, L.; Naji, L.; Palomar, J.; Omar, S.; Eser, S.; Rodriguez, J.; Álvarez-Montero, M.A. Deactivation behavior of Pd/C and Pt/C catalysts in the gas-phase hydrodechlorination of chloromethanes: Structure–reactivity relationship. *Appl. Catal. B Environ.* **2015**, *162*, 532–543. [CrossRef]
32. Fernandez-Ruiz, C.; Bedia, J.; Grau, J.M.; Romero, A.C.; Rodríguez, D.; Rodríguez, J.J.; Gómez-Sainero, L. Rodríguez Promoting Light Hydrocarbons Yield by Catalytic Hydrodechlorination of Residual Chloromethanes Using Palladium Supported on Zeolite Catalysts. *Catalysts* **2020**, *10*, 199. [CrossRef]
33. Gómez-Sainero, L.M.; Palomar, J.; Omar, S.; Fernández, C.; Bedia, J.; Álvarez-Montero, A.; Rodriguez, J.J. Valorization of chloromethanes by hydrodechlorination with metallic catalysts. *Catal. Today* **2018**, *310*, 75–85. [CrossRef]
34. Martin-Martinez, M.; Rodriguez, J.J.; Baker, R.T.; Gómez-Sainero, L.M. Deactivation and regeneration of activated carbon-supported Rh and Ru catalysts in the hydrodechlorination of chloromethanes into light olefins. *Chem. Eng. J.* **2020**, *397*, 125479. [CrossRef]
35. Álvarez-Montero, M.; Gómez-Sainero, L.; Mayoral, A.; Diaz, I.; Baker, R.; Rodriguez, J. Hydrodechlorination of chloromethanes with a highly stable Pt on activated carbon catalyst. *J. Catal.* **2011**, *279*, 389–396. [CrossRef]
36. Álvarez-Montero, M.A.; Gómez-Sainero, L.; Juan-Juan, J.; Linares-Solano, A.; Rodriguez, J. Gas-phase hydrodechlorination of dichloromethane with activated carbon-supported metallic catalysts. *Chem. Eng. J.* **2010**, *162*, 599–608. [CrossRef]
37. Martin-Martinez, M.; Gómez-Sainero, L.M.; Palomar, J.; Omar, S.; Rodriguez, J.J. Dechlorination of Dichloromethane by Hydrotreatment with Bimetallic Pd-Pt/C Catalyst. *Catal. Lett.* **2016**, *146*, 2614–2621. [CrossRef]
38. De Pedro, Z.M.; Casas, J.A.; Gomez-Sainero, L.M.; Rodriguez, J.J. Hydrodechlorination of dichloromethane with a Pd/AC catalyst: Reaction pathway and kinetics. *Appl. Catal. B Environ.* **2010**, *98*, 79–85. [CrossRef]
39. De Pedro, Z.M.; Gómez-Sainero, L.M.; González-Serrano, E.; Rodríguez, J.J. Gas-Phase Hydrodechlorination of Dichloromethane at Low Concentrations with Palladium/Carbon Catalysts. *Ind. Eng. Chem. Res.* **2006**, *45*, 7760–7766. [CrossRef]

40. Martino, M.; Rosal, R.; Sastre, H.; Díez, F.V. Hydrodechlorination of dichloromethane, trichloroethane, trichloroethylene and tetrachloroethylene over a sulfided Ni/Mo–γ-alumina catalyst. *Appl. Catal. B Environ.* **1999**, *20*, 301–307. [CrossRef]
41. Álvarez-Montero, M.A.; Rodriguez, J.J.; Gómez-Sainero, L.M. Platinum Nanoparticles Supported on Activated Carbon Catalysts for the Gas-Phase Hydrodechlorination of Dichloromethane: Influence of Catalyst Composition and Operating Conditions. *Nanomater. Nanotechnol.* **2016**, *6*, 18. [CrossRef]
42. Bedia, J.; Gómez-Sainero, L.; Grau, J.M.; Busto, M.; Martin-Martinez, M.; Rodriguez, J. Hydrodechlorination of dichloromethane with mono- and bimetallic Pd–Pt on sulfated and tungstated zirconia catalysts. *J. Catal.* **2012**, *294*, 207–215. [CrossRef]
43. Álvarez-Montero, M.A.; Martin-Martinez, M.; Gómez-Sainero, L.M.; Arevalo-Bastante, A.; Bedia, J.; Rodriguez, J.J. Kinetic Study of the Hydrodechlorination of Chloromethanes with Activated-Carbon-Supported Metallic Catalysts. *Ind. Eng. Chem. Res.* **2015**, *54*, 2023–2029. [CrossRef]
44. López, E.; Ordóñez, S.; Diez, F.V. Deactivation of a Pd/Al2O3 catalyst used in hydrodechlorination reactions: Influence of the nature of organochlorinated compound and hydrogen chloride. *Appl. Catal. B Environ.* **2006**, *62*, 57–65. [CrossRef]
45. Saadun, A.J.; Zichittella, G.; Paunovic, V.; Markaide-Aiastui, B.A.; Mitchell, S.; Pérez-Ramírez, J. Epitaxially Directed Iridium Nanostructures on Titanium Dioxide for the Selective Hydrodechlorination of Dichloromethane. *ACS Catal.* **2019**, *10*, 528–542. [CrossRef]
46. Arevalo-Bastante, A.; Martin-Martinez, M.; Álvarez-Montero, M.A.; Rodríguez, J.J.; Gómez-Sainero, L. Properties of Carbon-supported Precious Metals Catalysts under Reductive Treatment and Their Influence in the Hydrodechlorination of Dichloromethane. *Catalysts* **2018**, *8*, 664. [CrossRef]
47. Lee, S.R.; Cho, J.M.; Son, M.; Park, M.-J.; Kim, W.Y.; Kim, S.Y.; Bae, J.W. Selective hydrodechlorination of trichloromethane to dichloromethane over bimetallic Pt-Pd/KIT-6: Catalytic activity and reaction kinetics. *Chem. Eng. J.* **2018**, *331*, 556–569. [CrossRef]
48. Ruiz, C.F.; Bedia, J.; Andreoli, S.; Eser, S.; Rodríguez, J.J.; Gómez-Sainero, L. Selectivity to Olefins in the Hydrodechlorination of Chloroform with Activated Carbon-Supported Palladium Catalysts. *Ind. Eng. Chem. Res.* **2019**, *58*, 20592–20600. [CrossRef]
49. Fernandez-Ruiz, C.; Bedia, J.; Bonal, P.; Rodriguez, J.J.; Gómez-Sainero, L. Chloroform conversion into ethane and propane by catalytic hydrodechlorination with Pd supported on activated carbons from lignin. *Catal. Sci. Technol.* **2018**, *8*, 3926–3935. [CrossRef]
50. Prati, L. Reductive catalytic dehalogenation of light chlorocarbons. *Appl. Catal. B Environ.* **1999**, *23*, 135–142. [CrossRef]
51. Bae, J.W.; Lee, J.S.; Lee, K.H. Hydrodechlorination of CCl4 over Pt/γ-Al2O3 prepared from different Pt precursors. *Appl. Catal. A Gen.* **2008**, *334*, 156–167. [CrossRef]
52. Lokteva, E.S.; Lunin, V.V.; Golubina, E.V.; Simagina, V.I.; Egorova, M.; Stoyanova, I.V. C-C bond formation during hydrodechlorination of CCl4 on Pd-containing catalysts. *Adv. Pharmacol.* **2000**, *130*, 1997–2002. [CrossRef]
53. Bonarowska, M.; Wojciechowska, M.; Zieliński, M.; Kiderys, A.; Zieliński, M.; Winiarek, P.; Karpiński, Z. Hydrodechlorination of Tetrachloromethane over Palladium Catalysts Supported on Mixed MgF_2-MgO Carriers. *Molecules* **2016**, *21*, 1620. [CrossRef]
54. Cao, Y.C.; Jiang, X.Z. Supported platinum–gallium catalysts for selective hydrodechlorination of CCl_4. *J. Mol. Catal. A Chem.* **2005**, *242*, 119–128. [CrossRef]
55. Bonarowska, M.; Karpiński, Z. Hydrodechlorination of Tetrachloromethane Over Supported Platinum Catalysts. Effects of Hydrogen Partial Pressure and Catalyst's Screening Protocol on the Catalytic Performance. *Top. Catal.* **2012**, *55*, 846–852. [CrossRef]
56. Bae, J.W.; Park, E.D.; Lee, J.S.; Lee, K.H.; Kim, Y.G.; Yeon, S.H.; Sung, B.H. Hydrodechlorination of CCl_4 over Pt/γ-Al_2O_3. *Appl. Catal. A Gen.* **2001**, *217*, 79–89. [CrossRef]
57. Bae, J.W.; Jang, E.J.; Lee, B.I.; Lee, J.S.; Lee, K.H. Effects of Tin on Product Distribution and Catalyst Stability in Hydrodechlorination of CCl_4 over Pt-Sn/γ-Al_2O_3. *Ind. Eng. Chem. Res.* **2007**, *46*, 1721–1730. [CrossRef]
58. Lu, M.; Sun, J.; Zhang, D.; Li, M.; Zhu, J.; Shan, Y. Highly selective hydrodechlorination of CCl4 into CHCl3 on Ag–Pd/carbon catalysts. *React. Kinet. Mech. Catal.* **2010**, *100*, 99–103. [CrossRef]
59. Karpiński, Z.; Bonarowska, M.; Juszczyk, W. Hydrodechlorination of tetrachloromethane over silica-supported palladium-gold alloys. *Pol. J. Chem. Technol.* **2014**, *16*, 101–105. [CrossRef]

60. Bonarowska, M.; Kaszkur, Z.; Łomot, D.; Rawski, M.; Karpiński, Z. Effect of gold on catalytic behavior of palladium catalysts in hydrodechlorination of tetrachloromethane. *Appl. Catal. B Environ.* **2015**, *162*, 45–56. [CrossRef]
61. Bonarowska, M.; Karpiński, Z.; Kosydar, R.; Szumełda, T.; Drelinkiewicz, A. Hydrodechlorination of CCl_4 over carbon-supported palladium–gold catalysts prepared by the reverse "water-in-oil" microemulsion method. *Comptes Rendus Chim.* **2015**, *18*, 1143–1151. [CrossRef]
62. Molina, C.B.; Pizarro, A.H.; Casas, J.A.; Rodriguez, J.J. Enhanced Pd pillared clays by Rh inclusion for the catalytic hydrodechlorination of chlorophenols in water. *Water Sci. Technol.* **2012**, *65*, 653–660. [CrossRef]
63. Baeza, J.; Calvo, L.; Rodriguez, J.; Carbo-Argibay, E.; Rivas, J.; Gilarranz, M.A. Activity enhancement and selectivity tuneability in aqueous phase hydrodechlorination by use of controlled growth Pd-Rh nanoparticles. *Appl. Catal. B Environ.* **2015**, *168*, 283–292. [CrossRef]
64. Yuan, G.; Louis, C.; Delannoy, L.; Keane, M.A. Silica- and titania-supported Ni–Au: Application in catalytic hydrodechlorination. *J. Catal.* **2007**, *247*, 256–268. [CrossRef]
65. Legawiec-Jarzyna, M.; Juszczyk, W.; Bonarowska, M.; Kaszkur, Z.; Kępiński, L.; Kowalczyk, Z.; Karpiński, Z. Hydrodechlorination of CCl4 on Pt–Au/Al2O3 Catalysts. *Top. Catal.* **2009**, *52*, 1037–1043. [CrossRef]
66. Choi, H.C.; Choi, S.H.; Lee, J.S.; Lee, K.H.; Kim, Y.G. Effects of Pt Precursors on Hydrodechlorination of Carbon Tetrachloride over Pt/Al_2O_3. *J. Catal.* **1997**, *166*, 284–293. [CrossRef]
67. Zhang, Z.; Beard, B. Genesis of durable catalyst for selective hydrodechlorination of CCl_4 to $CHCl_3$. *Appl. Catal. A Gen.* **1998**, *174*, 33–39. [CrossRef]
68. Legawiec-Jarzyna, M.; Śrębowata, A.; Juszczyk, W. Hydrodechlorination of chloroalkanes on supported platinum catalysts. *React. Kinet. Catal. Lett.* **2006**, *87*, 291–296. [CrossRef]
69. Fási, A.; Hannus, I.; Halász, J.; Pálinkó, I. Hydrodechlorination Reactions of CCl4 Over HZSM-5- and HY-Supported Pt and Pd Catalysts. *Top. Catal.* **2012**, *55*, 853–857. [CrossRef]
70. Choi, H.C.; Choi, S.H.; Yang, O.B.; Lee, J.S.; Lee, K.H.; Kim, Y.G. Hydrodechlorination of Carbon Tetrachloride over Pt/MgO. *J. Catal.* **1996**, *161*, 790–797. [CrossRef]
71. Garetto, T.F.; Vignatti, C.; Borgna, A.; Monzón, A. Deactivation and regeneration of Pt/Al_2O_3 catalysts during the hydrodechlorination of carbon tetrachloride. *Appl. Catal. B Environ.* **2009**, *87*, 211–219. [CrossRef]
72. Gómez-Sainero, L.M.; Seoane, X.L.; Arcoya, A. Hydrodechlorination of carbon tetrachloride in the liquid phase on a Pd/carbon catalyst: Kinetic and mechanistic studies. *Appl. Catal. B Environ.* **2004**, *53*, 101–110. [CrossRef]
73. Legawiecjarzyna, M.; Śrębowata, A.; Juszczyk, W.; Karpinski, Z. Hydrodechlorination over $Pd–Pt/Al_2O_3$ catalysts. *Appl. Catal. A Gen.* **2004**, *271*, 61–68. [CrossRef]
74. De Souza, A.G.F.; Bentes, A.M.P., Jr.; Rodrigues, A.C.C.; Borges, L.E.P.; Monteiro, J.L.F. Hydrodechlorination of carbon tetrachloride over PtNaX zeolite: Deactivation studies. *Catal. Today* **2005**, *107-108*, 493–499. [CrossRef]
75. Golubina, E.V.; Lokteva, E.S.; Lunin, V.V.; O Turakulova, A.; Simagina, V.I.; Stoyanova, I.V. Modification of the supported palladium catalysts surface during hydrodechlorination of carbon tetrachloride. *Appl. Catal. A Gen.* **2003**, *241*, 123–132. [CrossRef]
76. Santo, V.D.; Dossi, C.; Recchia, S.; Colavita, P.; Vlaic, G.; Psaro, R. Carbon tetrachloride hydrodechlorination with organometallics-based platinum and palladium catalysts on MgO. *J. Mol. Catal. A Chem.* **2002**, *182–183*, 157–166. [CrossRef]
77. Machynskyy, O.; Śrębowata, A.; Kemnitz, E.; Karpiński, Z. Hydrodechlorination of Carbon Tetrachloride and 1,2-Dichloroethane on Palladium Nanoparticles Supported on Metal Fluorides. *Int. J. Green Energy* **2014**, *12*, 780–786. [CrossRef]
78. Lu, M.; Li, X.; Chen, B.; Li, M.; Xin, H.; Song, L. Catalytic dechlorination of carbon tetrachloride in liquid phase with methanol as H-donor over Ag/C catalyst. *J. Nanosci. Nanotechnol.* **2014**, *14*, 7315–7318. [CrossRef] [PubMed]
79. Delannoy, L.; Giraudon, J.-M.; Grangerc, P.; Leclercq, L.; Leclercq, G. Hydrodechlorination of CCl4 over group VI transition metal carbides. *Appl. Catal. B Environ.* **2002**, *37*, 161–173. [CrossRef]
80. Bonarowska, M.; Zieliński, M.; Matus, K.; Sá, J.; Śrębowata, A. Influence of microwave activation on the catalytic behavior of Pd-Au/C catalysts employed in the hydrodechlorination of tetrachloromethane. *React. Kinet. Mech. Catal.* **2018**, *124*, 375–388. [CrossRef]

81. Kim, S.Y.; Choi, H.C.; Yanga, O.B.; Lee, K.H.; Lee, J.S.; Kim, Y.G. Hydrodechlorination of tetrachloromethane over supported Pt catalysts. *J. Chem. Soc. Chem. Commun.* **1995**, *21*, 2169. [CrossRef]
82. Gómez-Sainero, L.M.; Seoane, X.L.; Tijero, E.; Arcoya, A. Hydrodechlorination of carbon tetrachloride to chloroform in the liquid phase with a Pd/carbon catalyst. Study of the mass transfer steps. *Chem. Eng. Sci.* **2002**, *57*, 3565–3574. [CrossRef]
83. Gomez-Sainero, L.M.; Cortés, A.; Seoane, X.L.; Arcoya, A. Hydrodechlorination of Carbon Tetrachloride to Chloroform in the Liquid Phase with Metal-Supported Catalysts. Effect of the Catalyst Components. *Ind. Eng. Chem. Res.* **2000**, *39*, 2849–2854. [CrossRef]
84. Ahmadzai, H.; Bock, R.P.; Burholder, J.B.; Butler, J.H.; Chatteriee, A.; Chipperfield, M.P.; Daniel, J.S.; Derek, N.; Fleming, E.L.; Fraser, P.J.; et al. *SPARC Report on the Mystery of Carbon Tetrachloride*; No. 7; WCRP: Geneva, Switzerland, 2016; pp. 1–67.
85. Martin-Martinez, M.; Gómez-Sainero, M.L.; Bedia, J.; Arevalo-Bastante, A.; Rodríguez, J.J. Enhanced activity of carbon-supported Pd–Pt catalysts in the hydrodechlorination of dichloromethane. *Appl. Catal. B Environ.* **2016**, *184*, 55–63. [CrossRef]
86. Keane, M.A. Supported Transition Metal Catalysts for Hydrodechlorination Reactions. *ChemCatChem* **2011**, *3*, 800–821. [CrossRef]
87. Mori, T.; Kikuchi, T.; Kubo, J.; Morikawa, Y. Hydrodechlorination of Trichloromethane to Higher Hydrocarbons over Pd/SiO_2 Catalyst. *Chem. Lett.* **2001**, *30*, 936–937. [CrossRef]
88. Ali, A.M.; Podila, S.; Daous, M.A.; Al-Zahrani, A.A.; Mahpudz, A. Highly efficient hydrotalcite supported palladium catalyst for hydrodechlorination of 1,2,4-tri chlorobenzene: Influence of Pd loading. *J. Chem. Sci.* **2020**, *132*, 1–10. [CrossRef]
89. Gómez-Sainero, L.M.; Seoane, X.L.; Fierro, J.L.; Arcoya, A. Liquid-Phase Hydrodechlorination of CCl4 to $CHCl_3$ on Pd/Carbon Catalysts: Nature and Role of Pd Active Species. *J. Catal.* **2002**, *209*, 279–288. [CrossRef]
90. Jujjuri, S.; Ding, E.; Hommel, E.; Shore, S.; Keane, M.A. Synthesis and characterization of novel silica-supported Pd/Yb bimetallic catalysts: Application in gas-phase hydrodechlorination and hydrogenation. *J. Catal.* **2006**, *239*, 486–500. [CrossRef]
91. Cao, Y.C.; Li, Y. In situ synthesis of supported palladium complexes: Highly stable and selective supported palladium catalysts for hydrodechlorination of CCl_2F_2. *Appl. Catal. A Gen.* **2005**, *294*, 298–305. [CrossRef]
92. Bonarowska, M.; Matus, K.; Śrębowata, A.; Sá, J. Application of silica-supported Ir and Ir-M (M = Pt, Pd, Au) catalysts for low-temperature hydrodechlorination of tetrachloromethane. *Sci. Total. Environ.* **2018**, *644*, 287–297. [CrossRef]
93. Golubina, E.V.; Lokteva, E.S.; Lazareva, T.S.; Kostyuk, B.G.; Lunin, V.V.; Simagina, V.I.; Stoyanova, I.V. Hydrodechlorination of Tetrachloromethane in the Vapor Phase in the Presence of Pd–Fe/Sibunit Catalysts. *Kinet. Catal.* **2004**, *45*, 183–188. [CrossRef]
94. Rodríguez-Reinoso, F.; Rodríguez-Ramos, I.; Moreno-Castilla, C.; Guerrero-Ruiz, A.; López-González, J.D. Platinum catalyst supported on activated carbons: I. Preparation and characterization. *J. Catal.* **1983**, *99*, 171–183. [CrossRef]
95. Ruiz-Garcia, C.; Heras, F.; Calvo, L.; Alonso-Morales, N.; Rodriguez, J.; Gilarranz, M. Improving the activity in hydrodechlorination of Pd/C catalysts by nitrogen doping of activated carbon supports. *J. Environ. Chem. Eng.* **2020**, *8*, 103689. [CrossRef]
96. Bonarowska, M.; Burda, B.; Juszczyk, W.; Pielaszek, J.; Kowalczyk, Z.; Karpinski, Z. Hydrodechlorination of CCl_2F_2 (CFC-12) over Pd-Au/C catalysts. *Appl. Catal. B Environ.* **2001**, *35*, 13–20. [CrossRef]
97. Amorim, C.; Yuan, G.; Patterson, P.M.; Keane, M.A. Catalytic hydrodechlorination over Pd supported on amorphous and structured carbon. *J. Catal.* **2005**, *234*, 268–281. [CrossRef]
98. Orellana, F.; Pecchi, G.; Reyes, P. Selective hydrodechlorination of 1,2-dichloroethane over Pd-Sn/SiO_2 catalysts. *J. Chil. Chem. Soc.* **2005**, *50*, 431–434. [CrossRef]
99. Ning, X.; Sun, Y.; Fu, H.; Qu, X.; Xu, Z.; Zheng, S. N-doped porous carbon supported Ni catalysts derived from modified Ni-MOF-74 for highly effective and selective catalytic hydrodechlorination of 1,2-dichloroethane to ethylene. *Chemosphere* **2020**, *241*, 124978. [CrossRef] [PubMed]
100. Merte, L.R.; Peng, G.; Bechstein, R.; Rieboldt, F.; Farberow, C.A.; Grabow, L.C.; Kudernatsch, W.; Wendt, S.; Laegsgaard, E.; Mavrikakis, M.; et al. Water-Mediated Proton Hopping on an Iron Oxide Surface. *Science* **2012**, *336*, 889–893. [CrossRef] [PubMed]

101. Karim, W.; Spreafico, C.; Kleibert, A.; Gobrecht, J.; Vandevondele, C.S.J.; Ekinci, W.K.J.G.Y.; Van Bokhoven, W.K.J.A. Catalyst support effects on hydrogen spillover. *Nat. Cell Biol.* **2017**, *541*, 68–71. [CrossRef] [PubMed]
102. Im, J.; Shin, H.; Jang, H.; Kim, H.; Choi, M. Maximizing the catalytic function of hydrogen spillover in platinum-encapsulated aluminosilicates with controlled nanostructures. *Nat. Commun.* **2014**, *5*, 3370. [CrossRef] [PubMed]
103. Haber, J.; Block, J.H.; Delmon, B. Manual of methods and procedures for catalyst characterization (Technical Report). *Pure Appl. Chem.* **1995**, *67*, 1257–1306. [CrossRef]
104. Ruiz, P.; Gaigneaux, E.; De Vos, D.E.; Martens, J.A.; Poncelet, G.; Jacobs, P.A. *Scientific Bases for the Preparation of Heterogeneous Catalysts*, 1st ed.; Elsevier Science: Amsterdam, The Netherlands, 2002.
105. Huang, Y.; Schwarz, J. The effect of catalyst preparation on catalytic activity. *Appl. Catal.* **1987**, *30*, 239–253. [CrossRef]
106. Gurbani, A.; Ayastuy, J.; González-Marcos, M.; Herrero, J.; Guil, J.; Gutiérrez-Ortiz, M.A. Comparative study of CuO–CeO2 catalysts prepared by wet impregnation and deposition–precipitation. *Int. J. Hydrog. Energy* **2009**, *34*, 547–553. [CrossRef]
107. Wu, Z.; Tang, N.; Xiao, L.; Liu, Y.; Wang, H. MnOx/TiO2 composite nanoxides synthesized by deposition-precipitation method as a superior catalyst for NO oxidation. *J. Colloid Interface Sci.* **2010**, *352*, 143–148. [CrossRef]
108. Bonarowska, M.; Karpiński, Z. Characterization of supported Pd-Pt catalysts by chemical probes. *Catal. Today* **2008**, *137*, 498–503. [CrossRef]
109. Imre, B.; Hannus, I.; Kiricsi, I. Comparative IR spectroscopic study of Pt- and Pd-containing zeolites in the hydrodechlorination reaction of carbon tetrachloride. *J. Mol. Struct.* **2005**, *744-747*, 501–506. [CrossRef]
110. Bradu, C.; Căpăţ, C.; Papa, F.; Frunza, L.; Olaru, E.-A.; Crini, G.; Morin-Crini, N.; Euvrard, É.; Balint, I.; Zgura, I.; et al. Pd-Cu catalysts supported on anion exchange resin for the simultaneous catalytic reduction of nitrate ions and reductive dehalogenation of organochlorinated pollutants from water. *Appl. Catal. A Gen.* **2019**, *570*, 120–129. [CrossRef]
111. Liu, Y.; Diao, X.; Tao, F.; Yang, C.; Wang, H.; Takaoka, M.; Sun, Y. Insight into the low-temperature decomposition of Aroclor 1254 over activated carbon-supported bimetallic catalysts obtained with XANES and DFT calculations. *J. Hazard. Mater.* **2019**, *366*, 538–544. [CrossRef] [PubMed]
112. Chang, W.; Kim, H.; Oh, J.; Ahn, B.J. Hydrodechlorination of chlorophenols over Pd catalysts supported on zeolite Y, MCM-41 and graphene. *Res. Chem. Intermed.* **2018**, *44*, 3835–3847. [CrossRef]
113. Kowalewski, E.; Kamińska, I.I.; Słowik, G.; Lisovytskiy, D.; Śrębowata, A. Effect of metal precursor and pretreatment conditions on the catalytic activity of Ni/C in the aqueous phase hydrodechlorination of 1,1,2-trichloroethene. *React. Kinet. Mech. Catal.* **2017**, *121*, 3–16. [CrossRef]
114. Terekhov, A.V.; Zanaveskin, L.N.; Zanaveskin, K.L.; Konorev, O.A. Catalytic hydrodechlorination of chlorinated hydrocarbons in a medium of sodium hydroxide solutions. I: Conversion of carbon tetrachloride. *Catal. Ind.* **2013**, *5*, 32–41. [CrossRef]
115. Ren, Y.; Fan, G.; Jiang, W.; Xu, B.; Liu, F. Effective hydrodechlorination of 4-chlorophenol catalysed by magnetic palladium/reduced graphene oxide under mild conditions. *RSC Adv.* **2014**, *4*, 25440–25446. [CrossRef]
116. Choi, E.-K.; Park, K.-H.; Lee, H.-B.; Cho, M.; Ahn, S. Formic acid as an alternative reducing agent for the catalytic nitrate reduction in aqueous media. *J. Environ. Sci.* **2013**, *25*, 1696–1702. [CrossRef]
117. Kopinke, F.-D.; MacKenzie, K.; Koehler, R.; Georgi, A. Alternative sources of hydrogen for hydrodechlorination of chlorinated organic compounds in water on Pd catalysts. *Appl. Catal. A Gen.* **2004**, *271*, 119–128. [CrossRef]
118. Liu, H.; Long, L.; Xu, Z.; Zheng, S. Pd-NCQD composite confined in SBA-15 as highly active catalyst for aqueous phase catalytic hydrodechlorination of 2,4-dichlorophenoxyacetic acid. *Chem. Eng. J.* **2020**, *400*, 125987. [CrossRef]
119. Feng, Z.; Gao, C.; Ma, X.; Zhan, J. Well-dispersed Pd nanoparticles on porous ZnO nanoplates via surface ion exchange for chlorobenzene-selective sensor. *RSC Adv.* **2019**, *9*, 42351–42359. [CrossRef]
120. Baeza, J.; Calvo, L.; Gilarranz, M.A.; Rodriguez, J. Effect of size and oxidation state of size-controlled rhodium nanoparticles on the aqueous-phase hydrodechlorination of 4-chlorophenol. *Chem. Eng. J.* **2014**, *240*, 271–280. [CrossRef]

121. Bonarowska, M.; Kaszkur, Z.; Kępiński, L.; Karpiński, Z. Hydrodechlorination of tetrachloromethane on alumina- and silica-supported platinum catalysts. *Appl. Catal. B Environ.* **2010**, *99*, 248–256. [CrossRef]
122. Ramos, A.L.D.; Alves, P.D.S.; Aranda, D.A.G.; Schmal, M. Characterization of carbon supported palladium catalysts: Inference of electronic and particle size effects using reaction probes. *Appl. Catal. A Gen.* **2004**, *277*, 71–81. [CrossRef]
123. Baeza, J.A.; Calvo, L.; Murzin, D.Y.; Rodriguez, J.J.; Gilarranz, M.A. Kinetic Analysis of 4-Chlorophenol Hydrodechlorination Catalyzed by Rh Nanoparticles Based on the Two-Step Reaction and Langmuir–Hinshelwood Mechanisms. *Catal. Lett.* **2014**, *144*, 2080–2085. [CrossRef]
124. Baeza, J.; Calvo, L.; Gilarranz, M.; Mohedano, A.; Casas, J.; Rodriguez, J. Catalytic behavior of size-controlled palladium nanoparticles in the hydrodechlorination of 4-chlorophenol in aqueous phase. *J. Catal.* **2012**, *293*, 85–93. [CrossRef]
125. Bae, J.W.; Kim, I.G.; Lee, J.S.; Lee, K.H.; Jang, E.J. Hydrodechlorination of CCl_4 over Pt/Al_2O_3: Effects of platinum particle size on product distribution. *Appl. Catal. A Gen.* **2003**, *240*, 129–142. [CrossRef]
126. Gómez-Quero, S.; Cárdenas-Lizana, F.; Keane, M.A. Effect of Metal Dispersion on the Liquid-Phase Hydrodechlorination of 2,4-Dichlorophenol over Pd/Al_2O_3. *Ind. Eng. Chem. Res.* **2008**, *47*, 6841–6853. [CrossRef]
127. Omar, S.; Palomar, J.; Gómez-Sainero, L.M.; Álvarez-Montero, M.A.; Martin-Martinez, M.; Rodriguez, J.J. Density Functional Theory Analysis of Dichloromethane and Hydrogen Interaction with Pd Clusters: First Step to Simulate Catalytic Hydrodechlorination. *J. Phys. Chem. C* **2011**, *115*, 14180–14192. [CrossRef]
128. Lv, X.; Prastistho, W.; Yang, Q.; Tokoro, C. Application of nano-scale zero-valent iron adsorbed on magnetite nanoparticles for removal of carbon tetrachloride: Products and degradation pathway. *Appl. Organomet. Chem.* **2020**, *34*, e5592. [CrossRef]
129. Lowry, G.V.; Reinhard, M. Hydrodehalogenation of 1- to 3-Carbon Halogenated Organic Compounds in Water Using a Palladium Catalyst and Hydrogen Gas. *Environ. Sci. Technol.* **1999**, *33*, 1905–1910. [CrossRef]
130. Huang, C.-C.; Lo, S.-L.; Lien, H.-L. Zero-valent copper nanoparticles for effective dechlorination of dichloromethane using sodium borohydride as a reductant. *Chem. Eng. J.* **2012**, *203*, 95–100. [CrossRef]
131. Huang, C.-C.; Lo, S.-L.; Lien, H.-L. Vitamin B12-mediated hydrodechlorination of dichloromethane by bimetallic Cu/Al particles. *Chem. Eng. J.* **2015**, *273*, 413–420. [CrossRef]
132. Karpiński, Z. Catalysis by Supported, Unsupported, and Electron-Deficient Palladium. *Adv. Catal.* **1990**, *37*, 45–100. [CrossRef]
133. He, Y.; Fan, J.; Feng, J.; Luo, C.; Yang, P.; Li, D. Pd nanoparticles on hydrotalcite as an efficient catalyst for partial hydrogenation of acetylene: Effect of support acidic and basic properties. *J. Catal.* **2015**, *331*, 118–127. [CrossRef]
134. Cecilia, J.A.; Infantes-Molina, A.; Rodríguez-Castellón, E.; Ilyina, A. Gas phase catalytic hydrodechlorination of chlorobenzene over cobalt phosphide catalysts with different P contents. *J. Hazard. Mater.* **2013**, *260*, 167–175. [CrossRef]
135. Padmasri, A.; Venugopal, A.; Kumar, V.S.; Shashikala, V.; Nagaraja, B.; Seetharamulu, P.; Sreedhar, B.; Raju, B.D.; Rao, P.K.; Rao, K.R. Role of hydrotalcite precursors as supports for Pd catalysts in hydrodechlorination of CCl_2F_2. *J. Mol. Catal. A Chem.* **2004**, *223*, 329–337. [CrossRef]
136. Celik, G.; Ailawar, S.A.; Gunduz, S.; Edmiston, P.L.; Ozkan, U.S. Formation of carbonaceous deposits on Pd-based hydrodechlorination catalysts: Vibrational spectroscopy investigations over Pd/Al_2O_3 and Pd/SOMS. *Catal. Today* **2019**, *323*, 129–140. [CrossRef]
137. Gerber, I.C.; Oubenali, M.; Bacsa, R.R.; Durand, J.; Gonçalves, A.G.; Pereira, M.; Jolibois, F.; Perrin, L.; Poteau, R.; Serp, P. Theoretical and Experimental Studies on the Carbon-Nanotube Surface Oxidation by Nitric Acid: Interplay between Functionalization and Vacancy Enlargement. *Chem A Eur. J.* **2011**, *17*, 11467–11477. [CrossRef]
138. Bonarowska, M.; Lin, K.N.; Jarzyna, M.L.; Stobinski, L.; Juszczyk, W.; Kaszkur, Z.; Karpiński, Z.; Lin, H.M. Multi-Wall Carbon Nanotubes as a Support for Platinum Catalysts for the Hydrodechlorination of Carbon Tetrachloride and Dichlorodifluoromethane. *Solid State Phenom.* **2007**, *128*, 261–271. [CrossRef]
139. Rosas, J.M.; Bedia, J.; Rodríguez-Mirasol, J.; Cordero, T. Preparation of Hemp-Derived Activated Carbon Monoliths. Adsorption of Water Vapor. *Ind. Eng. Chem. Res.* **2008**, *47*, 1288–1296. [CrossRef]
140. Bedia, J.; Rosas, J.M.; Márquez, J.; Rodríguez-Mirasol, J.; Cordero, T. Preparation and characterization of carbon based acid catalysts for the dehydration of 2-propanol. *Carbon* **2009**, *47*, 286–294. [CrossRef]

141. Valero-Romero, M.; García-Mateos, F.; Rodríguez-Mirasol, J.; Cordero, T. Role of surface phosphorus complexes on the oxidation of porous carbons. *Fuel Process. Technol.* **2017**, *157*, 116–126. [CrossRef]
142. Góralski, J.; Szczepaniak, B.; Grams, J.; Maniukiewicz, W.; Paryjczak, T. Characteristic of physicochemical properties of Pd/MgO catalysts used in the hydrodechlorination process with CCl_4. *Pol. J. Chem. Technol.* **2007**, *9*, 77–80. [CrossRef]
143. Lan, L.; Liu, Y.; Liu, S.; Ma, X.; Li, X.; Dong, Z.; Xia, C. Effect of the supports on catalytic activity of Pd catalysts for liquid-phase hydrodechlorination/hydrogenation reaction. *Environ. Technol.* **2019**, *40*, 1615–1623. [CrossRef]
144. Netskina, O.; Komova, O.; Tayban, E.; Oderova, G.; Mukha, S.; Kuvshinov, G.; Simagina, V.I. The influence of acid treatment of carbon nanofibers on the activity of palladium catalysts in the liquid-phase hydrodechlorination of dichlorobenzene. *Appl. Catal. A Gen.* **2013**, *467*, 386–393. [CrossRef]
145. Gerber, I.C.; Serp, P. A Theory/Experience Description of Support Effects in Carbon-Supported Catalysts. *Chem. Rev.* **2020**, *120*, 1250–1349. [CrossRef]
146. Karousis, N.; Tagmatarchis, N.; Tasis, D. Current Progress on the Chemical Modification of Carbon Nanotubes. *Chem. Rev.* **2010**, *110*, 5366–5397. [CrossRef]
147. Gu, X.; Qi, W.; Xu, X.; Sun, Z.; Zhang, L.; Liu, W.; Pan, X.; Su, D. Covalently functionalized carbon nanotube supported Pd nanoparticles for catalytic reduction of 4-nitrophenol. *Nanoscale* **2014**, *6*, 6609–6616. [CrossRef]
148. Kundu, S.; Wang, Y.; Xia, W.; Muhler, M. Thermal Stability and Reducibility of Oxygen-Containing Functional Groups on Multiwalled Carbon Nanotube Surfaces: A Quantitative High-Resolution XPS and TPD/TPR Study. *J. Phys. Chem. C* **2008**, *112*, 16869–16878. [CrossRef]
149. Shen, W.; Fan, W. Nitrogen-containing porous carbons: Synthesis and application. *J. Mater. Chem. A* **2013**, *1*, 999–1013. [CrossRef]
150. Cao, Y.; Mao, S.; Li, M.; Chen, Y.; Wang, Y. Metal/Porous Carbon Composites for Heterogeneous Catalysis: Old Catalysts with Improved Performance Promoted by N-Doping. *ACS Catal.* **2017**, *7*, 8090–8112. [CrossRef]
151. An, N.; Zhang, M.; Zhang, Z.; Dai, Y.; Shen, Y.; Tang, C.; Yuan, X.; Zhou, W. High-performance palladium catalysts for the hydrogenation toward dibenzylbiotinmethylester: Effect of carbon support functionalization. *J. Colloid Interface Sci.* **2018**, *510*, 181–189. [CrossRef]
152. Lu, C.; Wang, M.; Feng, Z.; Qi, Y.; Feng, F.; Ma, L.; Zhang, Q.; Li, X. A phosphorus–carbon framework over activated carbon supported palladium nanoparticles for the chemoselective hydrogenation of para-chloronitrobenzene. *Catal. Sci. Technol.* **2017**, *7*, 1581–1589. [CrossRef]
153. An, N.; Dai, Y.; Tang, C.; Yuan, X.; Dong, J.; Shen, Y.; Zhou, W. Design and preparation of a simple and effective palladium catalyst and the hydrogenation performance toward dibenzylbiotinmethylester. *J. Colloid Interface Sci.* **2016**, *470*, 56–61. [CrossRef]
154. Diaz, E.; Mohedano, A.F.; Casas, J.A.; Rodriguez, J.J. Analysis of the deactivation of Pd, Pt and Rh on activated carbon catalysts in the hydrodechlorination of the MCPA herbicide. *Appl. Catal. B Environ.* **2016**, *181*, 429–435. [CrossRef]
155. Bedia, J.; Rosas, J.; Rodríguez-Mirasol, J.; Cordero, T. Pd supported on mesoporous activated carbons with high oxidation resistance as catalysts for toluene oxidation. *Appl. Catal. B Environ.* **2010**, *94*, 8–18. [CrossRef]
156. Guillén, E.; Rico, R.; Lopezromero, J.M.; Bedia, J.; Rosas, J.M.; Rodríguez-Mirasol, J.; Cordero, T. Pd-activated carbon catalysts for hydrogenation and Suzuki reactions. *Appl. Catal. A Gen.* **2009**, *368*, 113–120. [CrossRef]
157. Chary, K.V.; Rao, P.V.R.; Vishwanathan, V. Synthesis and high performance of ceria supported nickel catalysts for hydrodechlorination reaction. *Catal. Commun.* **2006**, *7*, 974–978. [CrossRef]
158. Li, F.; Liu, Y.; Ma, T.; Xu, D.; Li, X.; Gong, G. Catalysis of the hydrodechlorination of 4-chlorophenol and the reduction of 4-nitrophenol by Pd/Fe_3O_4@C. *New J. Chem.* **2017**, *41*, 4014–4021. [CrossRef]
159. Concibido, N.C.; Okuda, T.; Nishijima, W.; Okada, M. Deactivation and reactivation of Pd/C catalyst used in repeated batch hydrodechlorination of PCE. *Appl. Catal. B Environ.* **2007**, *71*, 64–69. [CrossRef]
160. Bonarowska, M.; Malinowski, A.; Karpinski, Z. Hydrogenolysis of C–C and C–Cl bonds by Pd–Re/Al2O3 catalysts. *Appl. Catal. A Gen.* **1999**, *188*, 145–154. [CrossRef]
161. Chen, N.; Rioux, R.M.; Barbosa, L.A.M.M.; Ribeiro, F.H. Kinetic and Theoretical Study of the Hydrodechlorination of $CH_{4-x}Cl_x$ (x = 1−4) Compounds on Palladium†. *Langmuir* **2010**, *26*, 16615–16624. [CrossRef]
162. Reeves, C.; Meyer, R.; Mullins, C.B. Dissociative adsorption and hydrodechlorination of CCl4 on Ir(1 1 0). *J. Mol. Catal. A Chem.* **2003**, *202*, 135–146. [CrossRef]

163. Thomas, J.M.; Thomas, W.J. The Dynamics of Selective and Polyfunctional Catalysis. In *Introduction to the Principles of Heterogeneous Catalysts*; Thomas, J.M., Thomas, W.J., Eds.; Academic Press: New York, NY, USA, 1969; Chapter 7.
164. Centi, G. *Elementary Reaction Steps in Heterogeneous Catalysis*; Kluwer Academic Publishers: Dordrecht, The Netherlands, 1993; p. 93.
165. Converti, A.; Zilli, M.; De Faveri, D.M.; Ferraiolo, G. Hydrogenolysis of organochlorinated pollutants: Kinetics and thermodynamics. *J. Hazard. Mater.* **1991**, *27*, 127–135. [CrossRef]
166. Forni, P.; Prati, L.; Rossi, M. Catalytic dehydrohalogenation of polychlorinated biphenyls Part II: Studies on a continuous process. *Appl. Catal. B Environ.* **1997**, *14*, 49–53. [CrossRef]
167. Bartholomew, C.H. Mechanisms of catalyst deactivation. *Appl. Catal. A Gen.* **2001**, *212*, 17–60. [CrossRef]
168. Ordonez, S. Characterisation of the deactivation of platinum and palladium supported on activated carbon used as hydrodechlorination catalysts. *Appl. Catal. B Environ.* **2001**, *31*, 113–122. [CrossRef]
169. Urbano, F.J.; Marinas, J. Hydrogenolysis of organohalogen compounds over palladium supported catalysts. *J. Mol. Catal. A Chem.* **2001**, *173*, 329–345. [CrossRef]
170. Heinrichs, B. Palladium–silver sol–gel catalysts for selective hydrodechlorination of 1,2-dichloroethane into ethylene IV. Deactivation mechanism and regeneration. *J. Catal.* **2003**, *220*, 215–225. [CrossRef]
171. Chakraborty, D.; Kulkarni, P.P.; Kovalchuk, V.I.; D'Itri, J.L. Dehalogenative oligomerization of dichlorodifluoromethane catalyzed by activated carbon-supported Pt–Cu catalysts: Effect of Cu to Pt atomic ratio. *Catal. Today* **2004**, *88*, 169–181. [CrossRef]
172. Ordóñez, S.; Díaz, E.; Bueres, R.F.; Asedegbega-Nieto, E.; Sastre, H. Carbon nanofibre-supported palladium catalysts as model hydrodechlorination catalysts. *J. Catal.* **2010**, *272*, 158–168. [CrossRef]
173. Lapierre, R.B.; Wu, D.; Kranich, W.L.; Weiss, A.H. Hydrodechlorination of 1,1-bis(p-chlorophenyl)-2, 2-dichloroethylene (p,p'-DDE) in the vapor phase. *J. Catal.* **1978**, *52*, 59–71. [CrossRef]
174. Coq, B. Conversion of chlorobenzene over palladium and rhodium catalysts of widely varying dispersion. *J. Catal.* **1986**, *101*, 434–445. [CrossRef]
175. Fung, S. Hydrogenolysis of methyl chloride on metals. *J. Catal.* **1987**, *103*, 220–223. [CrossRef]
176. Gampine, A.; Eyman, D.P. Catalytic Hydrodechlorination of Chlorocarbons. 2. Ternary Oxide Supports for Catalytic Conversions of 1,2-Dichlorobenzene. *J. Catal.* **1998**, *179*, 315–325. [CrossRef]
177. Ordóñez, S.; Sastre, H.; Díez, F. Thermogravimetric determination of coke deposits on alumina-supported noble metal catalysts used as hydrodechlorination catalysts. *Thermochim. Acta* **2001**, *379*, 25–34. [CrossRef]
178. Aramendía, M.; Boráu, V.; García, I.; Jiménez, C.; Lafont, F.; Marinas, A.; Marinas, J.; Urbano, F.J. Liquid-phase hydrodechlorination of chlorobenzene over palladium-supported catalysts. *J. Mol. Catal. A Chem.* **2002**, *184*, 237–245. [CrossRef]
179. Tavoularis, G.; Keane, M.A. Gas phase catalytic dehydrochlorination and hydrodechlorination of aliphatic and aromatic systems. *J. Mol. Catal. A Chem.* **1999**, *142*, 187–199. [CrossRef]
180. Barrabés, N.; Föttinger, K.; Llorca, J.; Dafinov, A.; Medina, F.; Sá, J.; Hardacre, C.; Rupprechter, G.; Föttinger, K. Pretreatment Effect on Pt/CeO2 Catalyst in the Selective Hydrodechlorination of Trichloroethylene. *J. Phys. Chem. C* **2010**, *114*, 17675–17682. [CrossRef]
181. Kalmykov, P.A.; Magdalinova, N.A.; Klyuev, M.V. Liquid-Phase Hydrogenation of Halobenzenes in the Presence of Palladium-Containing Nanodiamonds. *Pet. Chem.* **2018**, *58*, 1206–1212. [CrossRef]
182. Rajagopal, S.; Spatola, A.F. Mechanism of Palladium-Catalyzed Transfer Hydrogenolysis of Aryl Chlorides by Formate Salts. *J. Org. Chem.* **1995**, *60*, 1347–1355. [CrossRef]
183. Aramendía, M.; Borau, V.; García, I.; Jimenez, C.; Marinas, J.; Urbano, F.J. Influence of the reaction conditions and catalytic properties on the liquid-phase hydrodebromination of bromobenzene over palladium supported catalysts: Activity and deactivation. *Appl. Catal. B Environ.* **1999**, *20*, 101–110. [CrossRef]
184. Park, C.; Menini, C.; Valverde, J.; Keane, M.A. Carbon–Chlorine and Carbon–Bromine Bond Cleavage in the Catalytic Hydrodehalogenation of Halogenated Aromatics. *J. Catal.* **2002**, *211*, 451–463. [CrossRef]
185. Dodson, D.A.; Rase, H.F. Methylene Chloride from Chloroform by Hydrochlorination. *Ind. Eng. Chem. Prod. Res. Dev.* **1978**, *17*, 236–240. [CrossRef]
186. Ordóñez, S.; Diez, F.V.; Sastre, H. Hydrodechlorination of tetrachloroethylene over vanadium-modified Pt/Al2O3 catalysts. *Catal. Lett.* **2001**, *72*, 177–182. [CrossRef]
187. Ordóñez, S.; Sastre, H.; Díez, F.V. Hydrodechlorination of tetrachloroethene over Pd/Al_2O_3: Influence of process conditions on catalyst performance and stability. *Appl. Catal. B Environ.* **2003**, *40*, 119–130. [CrossRef]

188. Moon, D.J.; Chung, M.J.; Park, K.Y.; Hong, S.I. Deactivation of Pd catalysts in the hydrodechlorination of chloropentafluoroethane. *Appl. Catal. A Gen.* **1998**, *168*, 159–170. [CrossRef]
189. Mori, T.; Yasuoka, T.; Morikawa, Y. Hydrodechlorination of 1,1,2-trichloro-1,2,2-trifluoroethane (CFC-113) over supported ruthenium and other noble metal catalysts. *Catal. Today* **2004**, *88*, 111–120. [CrossRef]
190. Coq, B.; Hub, S.; Figueras, F.; Tournigant, D. Conversion under hydrogen of dichlorodifluoromethane over bimetallic palladium catalysts. *Appl. Catal. A Gen.* **1993**, *101*, 41–50. [CrossRef]
191. Creyghton, E.; Burgers, M.; Jansen, J.; Van Bekkum, H. Vapour-phase hydrodehalogenation of chlorobenzene over platinum/H-BEA zeolite. *Appl. Catal. A Gen.* **1995**, *128*, 275–288. [CrossRef]
192. Van De Sandt, E.J.; Wiersma, A.; Makkee, M.; Van Bekkum, H.; Moulijn, J.A. Selection of activated carbon for the selective hydrogenolysis of CCl_2F_2 (CFC-12) into CH_2F_2 (HFC-32) over palladium-supported catalysts. *Appl. Catal. A Gen.* **1998**, *173*, 161–173. [CrossRef]
193. Mori, T.; Kubo, J.; Morikawa, Y. Hydrodechlorination of 1,1,1-trichloroethane over silica-supported palladium catalyst. *Appl. Catal. A Gen.* **2004**, *271*, 69–76. [CrossRef]
194. Ordóñez, S.; Díaz, E.; Díez, F.V.; Sastre, H. Regeneration of Pd/Al2O3 catalysts used for tetrachloroethylene hydrodechlorination. *React. Kinet. Catal. Lett.* **2007**, *90*, 101–106. [CrossRef]
195. Nieto-Márquez, A.; Valverde, J.; Keane, M.A. Catalytic growth of structured carbon from chloro-hydrocarbons. *Appl. Catal. A Gen.* **2007**, *332*, 237–246. [CrossRef]
196. Patrick, J.; Barranco, R. Carbon deposits: Formation, Nature and Characterization. In Proceedings of the COMA/CRF Meeting, Scunthorpe, UK, 27 April 2006.
197. Wiersma, A.; Van De Sandt, E.; Makkee, M.; Luteijn, C.; Van Bekkum, H.; Moulijn, J. Process for the selective hydrogenolysis of CCl2F2 (CFC-12) into CH2F2 (HFC-32). *Catal. Today* **1996**, *27*, 257–264. [CrossRef]
198. Makkee, M.; Van De Sandt, E.; Wiersma, A.; Moulijn, J. Development of a satisfactory palladium on activated carbon catalyst for the selective hydrogenolysis of CCl_2F_2 (CFC-12) into CH_2F_2 (HFC-32). *J. Mol. Catal. A Chem.* **1998**, *134*, 191–200. [CrossRef]
199. Kang, Y.; Han, Y.; Tian, M.; Huang, C.; Wang, C.; Lin, J.; Hou, B.; Su, Y.; Li, L.; Wang, J.; et al. Promoted methane conversion to syngas over Fe-based garnets via chemical looping. *Appl. Catal. B Environ.* **2020**, *278*, 119305. [CrossRef]
200. Yasuda, S.; Osuga, R.; Kunitake, Y.; Kato, K.; Fukuoka, A.; Kobayashi, H.; Gao, M.; Hasegawa, J.-Y.; Manabe, R.; Shima, H.; et al. Zeolite-supported ultra-small nickel as catalyst for selective oxidation of methane to syngas. *Commun. Chem.* **2020**, *3*, 1–8. [CrossRef]
201. Schwarz, H. Chemistry with Methane: Concepts Rather than Recipes. *Angew. Chem. Int. Ed.* **2011**, *50*, 10096–10115. [CrossRef]
202. Zhang, Q.; Wang, J.; Wang, T. Enhancing the Acetylene Yield from Methane by Decoupling Oxidation and Pyrolysis Reactions: A Comparison with the Partial Oxidation Process. *Ind. Eng. Chem. Res.* **2016**, *55*, 8383–8394. [CrossRef]
203. Dinh, D.K.; Lee, D.H.; Song, Y.-H.; Jo, S.; Kim, K.-T.; Iqbal, M.; Kang, H. Efficient methane-to-acetylene conversion using low-current arcs. *RSC Adv.* **2019**, *9*, 32403–32413. [CrossRef]
204. Velazquez, J.C.; Leekumjorn, S.; Nguyen, Q.X.; Fang, Y.-L.; Heck, K.N.; Hopkins, G.D.; Reinhard, M.; Wong, M.S. Chloroform hydrodechlorination behavior of alumina-supported Pd and PdAu catalysts. *AIChE J.* **2013**, *59*, 4474–4482. [CrossRef]
205. Xu, L.; Yao, X.; Khan, A.; Mavrikakis, M. Chloroform Hydrodechlorination over Palladium-Gold Catalysts: A First-Principles DFT Study. *ChemCatChem* **2016**, *8*, 1739–1746. [CrossRef]
206. Zhang, W.; Xu, S.; Zhi, Y.; Wei, Y.; Liu, Z. Methylcyclopentenyl cation mediated reaction route in methanol-to-olefins reaction over H-RUB-50 with small cavity. *J. Energy Chem.* **2020**, *45*, 25–30. [CrossRef]
207. Ebrahimi, A.; Haghighi, M.; Aghamohammadi, S. Effect of calcination temperature and composition on the spray-dried microencapsulated nanostructured SAPO-34 with kaolin for methanol conversion to ethylene and propylene in fluidized bed reactor. *Microporous Mesoporous Mater.* **2020**, *297*, 110046. [CrossRef]
208. Holmen, A. Direct conversion of methane to fuels and chemicals. *Catal. Today* **2009**, *142*, 2–8. [CrossRef]
209. Salih, H.A.; Muraza, O.; Abussaud, B.; Al-Shammari, T.K.; Yokoi, T. Catalytic Enhancement of SAPO-34 for Methanol Conversion to Light Olefins Using in Situ Metal Incorporation. *Ind. Eng. Chem. Res.* **2018**, *57*, 6639–6646. [CrossRef]
210. Wei, Y.; Zhang, D.; Liu, Z.; Su, B.-L. Methyl Halide to Olefins and Gasoline over Zeolites and SAPO Catalysts: A New Route of MTO and MTG. *Chin. J. Catal.* **2012**, *33*, 11–21. [CrossRef]

211. Zheng, J.; Jin, D.; Liu, Z.; Zhu, K.; Zhou, X.; Yuan, W.-K. Synthesis of Nanosized SAPO-34 via an Azeotrope Evaporation and Dry Gel Conversion Route and Its Catalytic Performance in Chloromethane Conversion. *Ind. Eng. Chem. Res.* **2018**, *57*, 548–558. [CrossRef]
212. Gosh, A.; Gosh, K.; Khanmamedova, A.; Mier, M.; Banke, J. Silicoaluminophosphate Catalyst for Chloromethane Conversion. Patent WO 2016/099775, 23 June 2016.
213. Fickel, D.W.; Sabnis, K.D.; Li, L.; Kulkarni, N.; Winter, L.R.; Yan, B.; Chen, J.G. Chloromethane to olefins over H-SAPO-34: Probing the hydrocarbon pool mechanism. *Appl. Catal. A Gen.* **2016**, *527*, 146–151. [CrossRef]
214. Zheng, J.; Zhang, W.; Liu, Z.; Huo, Q.; Zhu, K.; Zhou, X.; Yuan, W. Unraveling the non-classic crystallization of SAPO-34 in a dry gel system towards controlling meso-structure with the assistance of growth inhibitor: Growth mechanism, hierarchical structure control and catalytic properties. *Microporous Mesoporous Mater.* **2016**, *225*, 74–87. [CrossRef]
215. Kong, L.-T.; Shen, B.; Jiang, Z.; Zhao, J.-G.; Liu, J.-C. Synthesis of SAPO-34 with the presence of additives and their catalytic performance in the transformation of chloromethane to olefins. *React. Kinet. Mech. Catal.* **2015**, *114*, 697–710. [CrossRef]
216. Jiang, Z.; Shen, B.-X.; Zhao, J.-G.; Wang, L.; Kong, L.-T.; Xiao, W.-G. Enhancement of Catalytic Performances for the Conversion of Chloromethane to Light Olefins over SAPO-34 by Modification with Metal Chloride. *Ind. Eng. Chem. Res.* **2015**, *54*, 12293–12302. [CrossRef]
217. Kong, L.-T.; Jiang, Z.; Zhao, J.; Liu, J.; Shen, B. The Synthesis of Hierarchical SAPO-34 and its Enhanced Catalytic Performance in Chloromethane Conversion to Light Olefins. *Catal. Lett.* **2014**, *144*, 1609–1616. [CrossRef]
218. Olsbye, U.; Saure, O.V.; Muddada, N.B.; Bordiga, S.; Lamberti, C.; Nilsen, M.H.; Lillerud, K.P.; Svelle, S. Methane conversion to light olefins—How does the methyl halide route differ from the methanol to olefins (MTO) route? *Catal. Today* **2011**, *171*, 211–220. [CrossRef]
219. Shin, Y.H.; Kweon, S.; Park, M.B.; Chae, H.-J. Comparative study of CHA- and AEI-type zeolytic catalysts for the conversion of chloromethane into light olefins. *Korean J. Chem. Eng.* **2018**, *35*, 1433–1440. [CrossRef]
220. Gamero, M.; Aguayo, A.T.; Ateka, A.; Pérez-Uriarte, P.; Gayubo, A.G.; Bilbao, J. Role of Shape Selectivity and Catalyst Acidity in the Transformation of Chloromethane into Light Olefins. *Ind. Eng. Chem. Res.* **2015**, *54*, 7822–7832. [CrossRef]
221. Kong, L.-T.; Shen, B.-X.; Zhao, J.-G.; Liu, J.-C. Comparative Study on the Chloromethane to Olefins Reaction over SAPO-34 and HZSM-22. *Ind. Eng. Chem. Res.* **2014**, *53*, 16324–16331. [CrossRef]
222. Xu, T.; Liu, H.; Zhao, Q.; Cen, S.; Du, L.; Tang, Q. Conversion of chloromethane to propylene over fluoride-treated H-ZSM-35 zeolite catalysts. *Catal. Commun.* **2019**, *119*, 96–100. [CrossRef]
223. Huang, J.; Wang, W.; Fei, Z.; Liu, Q.; Chen, X.; Zhang, Z.; Tang, J.; Cui, M.; Qiao, X. Enhanced Light Olefin Production in Chloromethane Coupling over Mg/Ca Modified Durable HZSM-5 Catalyst. *Ind. Eng. Chem. Res.* **2019**, *58*, 5131–5139. [CrossRef]
224. Wen, D.; Liu, Q.; Fei, Z.; Yang, Y.; Zhang, Z.; Chen, X.; Tang, J.; Cui, M.; Qiao, X. Organosilane-Assisted Synthesis of Hierarchical Porous ZSM-5 Zeolite as a Durable Catalyst for Light-Olefins Production from Chloromethane. *Ind. Eng. Chem. Res.* **2018**, *57*, 446–455. [CrossRef]
225. Gamero, M.; Valle, B.; Castano, P.; Aguayo, A.T.; Bilbao, J. Reaction network of the chloromethane conversion into light olefins using a HZSM-5 zeolite catalyst. *J. Ind. Eng. Chem.* **2018**, *61*, 427–436. [CrossRef]
226. Liu, Q.; Wen, D.; Yang, Y.; Fei, Z.; Zhang, Z.; Chen, X.; Tang, J.; Cui, M.; Qiao, X. Enhanced catalytic performance for light-olefins production from chloromethane over hierarchical porous ZSM-5 zeolite synthesized by a growth-inhibition strategy. *Appl. Surf. Sci.* **2018**, *435*, 945–952. [CrossRef]
227. Gamero, M.; Valle, B.; Gayubo, A.G.; Castano, P.; Aguayo, A.T.; Bilbao, J. Kinetic Model for the Conversion of Chloromethane into Hydrocarbons over a HZSM-5 Zeolite Catalyst. *Ind. Eng. Chem. Res.* **2018**, *57*, 908–919. [CrossRef]
228. Ibáñez, M.; Gamero, M.; Ruiz-Martínez, J.J.; Weckhuysen, B.M.; Aguayo, A.T.; Bilbao, J.; Castano, P. Simultaneous coking and dealumination of zeolite H-ZSM-5 during the transformation of chloromethane into olefins. *Catal. Sci. Technol.* **2016**, *6*, 296–306. [CrossRef]
229. Xu, T.; Song, H.; Deng, W.; Zhang, Q.; Wang, Y. Catalytic conversion of methyl chloride to lower olefins over modified H-ZSM-34. *Chin. J. Catal.* **2013**, *34*, 2047–2056. [CrossRef]
230. Xu, T.; Zhang, Q.; Song, H.; Wang, Y. Fluoride-treated H-ZSM-5 as a highly selective and stable catalyst for the production of propylene from methyl halides. *J. Catal.* **2012**, *295*, 232–241. [CrossRef]

231. He, J.; Xu, T.; Wang, Z.; Zhang, Q.; Deng, W.; Wang, Y. Transformation of Methane to Propylene: A Two-Step Reaction Route Catalyzed by Modified CeO2 Nanocrystals and Zeolites. *Angew. Chem. Int. Ed.* **2012**, *51*, 2438–2442. [CrossRef]
232. Lokteva, E.S.; Simagina, V.I.; Golubina, E.V.; Stoyanova, I.V.; Lunin, V.V. Formation of C1–C5 Hydrocarbons from CCl4 in the Presence of Carbon-Supported Palladium Catalysts. *Kinet. Catal.* **2000**, *41*, 776–781. [CrossRef]
233. Mori, T.; Hirose, K.; Kikuchi, T.; Kubo, J.; Morikawa, Y. Formation of Higher Hydrocarbons from Chloromethanes via Hydrodechlorination over Pd/SiO_2 Catalyst. *J. Jpn. Pet. Inst.* **2002**, *45*, 256–259. [CrossRef]
234. Elola, A.; Díaz, E.; Ordóñez, S.; Díaz, E. A New Procedure for the Treatment of Organochlorinated Off-Gases Combining Adsorption and Catalytic Hydrodechlorination. *Environ. Sci. Technol.* **2009**, *43*, 1999–2004. [CrossRef] [PubMed]